LIGO–Virgo–KAGRA webinar

The population of merging compact binaries inferred using gravitational waves through GWTC-3

10 December 2021

Webinar streaming live from **15:00 UTC**

Image credit: LIGO/Caltech/MIT/Sonoma State/Aurore Simonnet

The population of merging compact binaries inferred using gravitational waves through GWTC-3

arXiv:2111.03634 •

15:00 UTC • 10 December 2021 • dcc.ligo.org/G2102458/public

GWTC-3 webinars

https://www.youtube.com/ligovirgo

6 December 2021: Compact binary coalescences observed by LIGO and Virgo during the second part of the third observing run

9 December 2021: Constraints on the cosmic expansion history from GWTC-3

Today: The population of merging compact binaries inferred using gravitational waves through GWTC-3

January 2022: Tests of general relativity with GWTC-3

LIGO VIRGO KAGRA

Speakers

Amanda Farah U Chicago	The Binary Merger Population
Philippe Landry CITA	Neutron Star Mergers
Vaibhav Tiwari Cardiff	Black Hole Masses
Tom Callister CCA	Black Hole Redshifts and Spins
Richard O'Shaughnessy RIT	Moderator Q&A

LIGO VIRGO KAGRA

Panelists

Fabio Antonini Cardiff University	Astro interpretation
Bruce Edelman University of Oregon	Black Hole Masses
Stephen Fairhurst Cardiff University	Additional events
Adrian Helmling-Cornell University of Oregon	Event selection
Jacob Golomb Caltech	Populations
Dan Wysocki UWM	Populations
Shanika Galaudage OzGrav/Monash University	Populations

Introduction Inputs Methods

Full Spectrum of Mergers

BNS and NSBH

BBH Mass

BBH Redshift and Spin

A Growing Catalog : GWTC-1

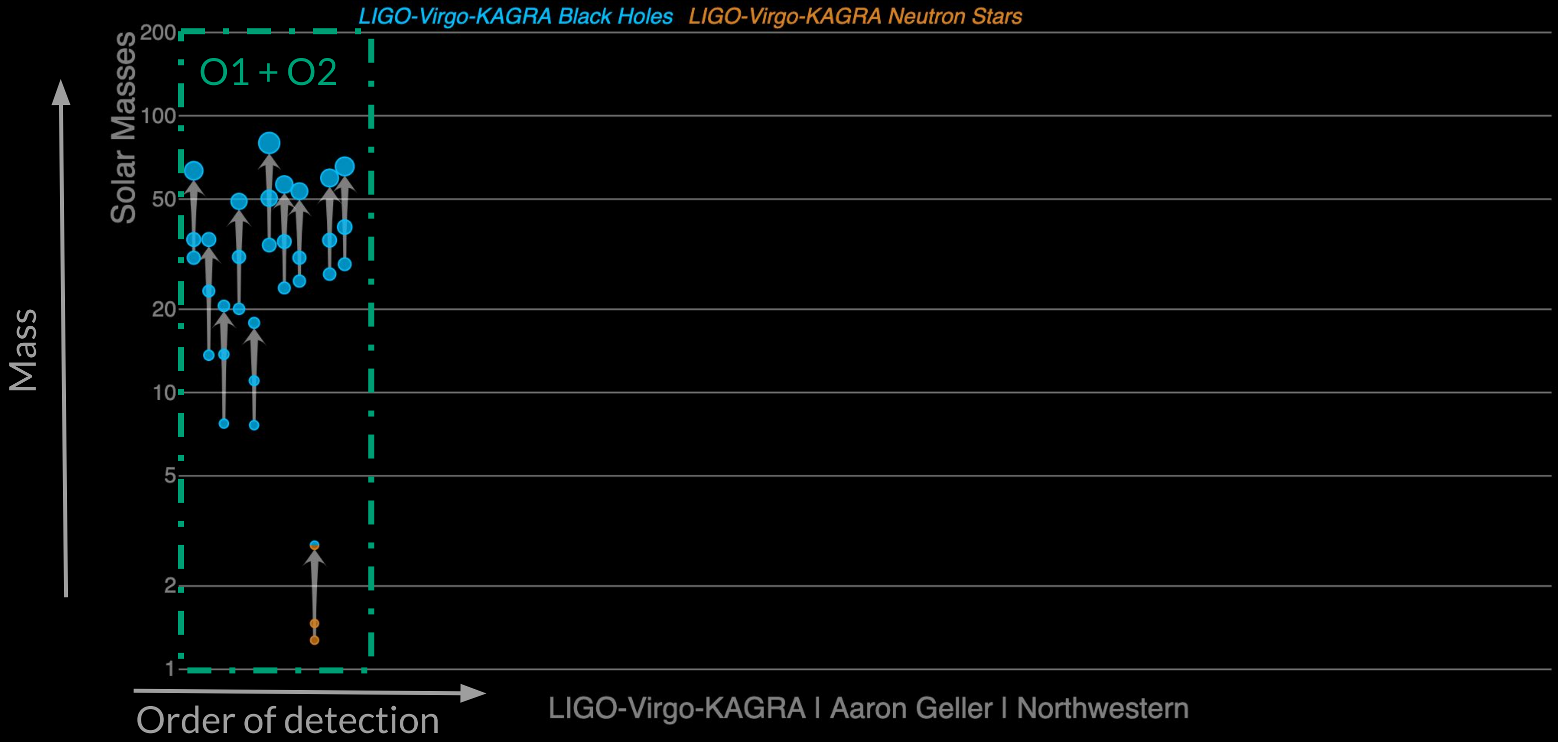

A Growing Catalog : GWTC-2.1

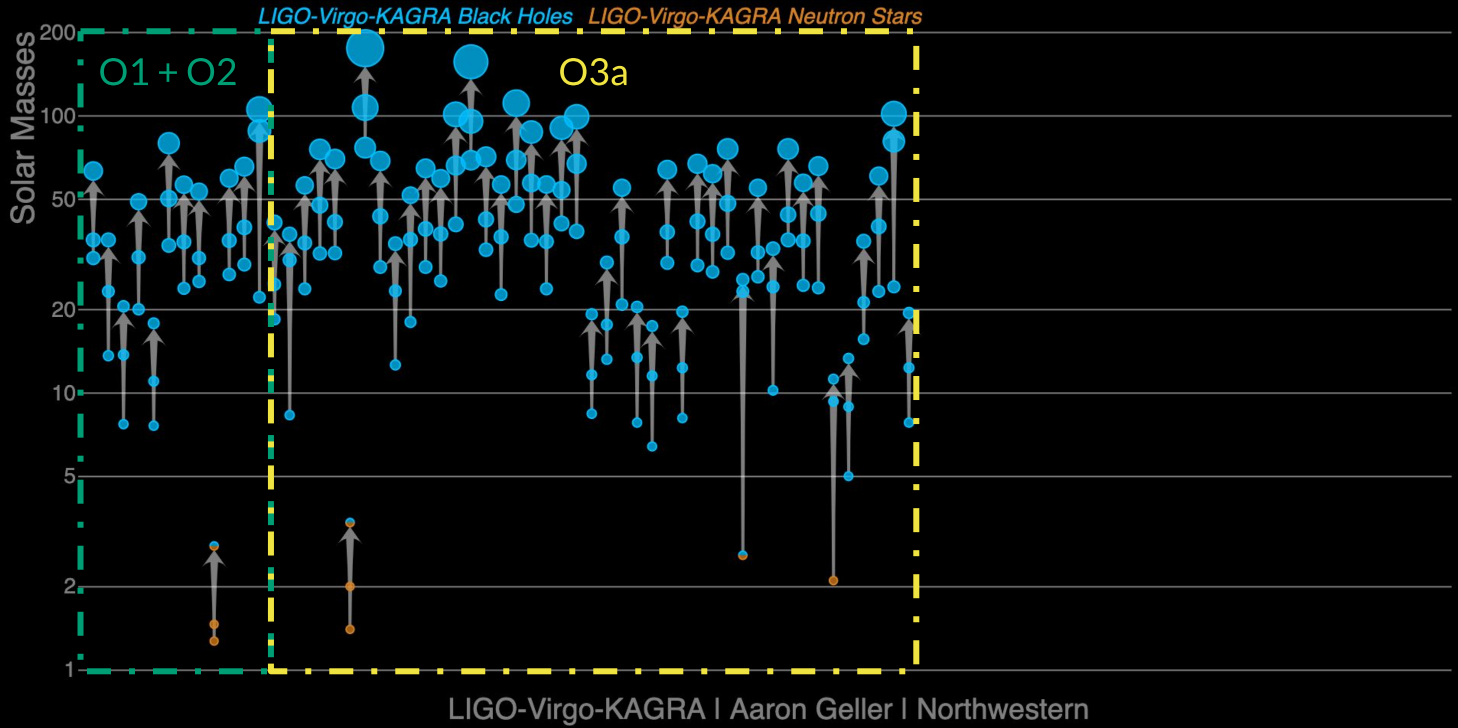

A Growing Catalog : GWTC-3

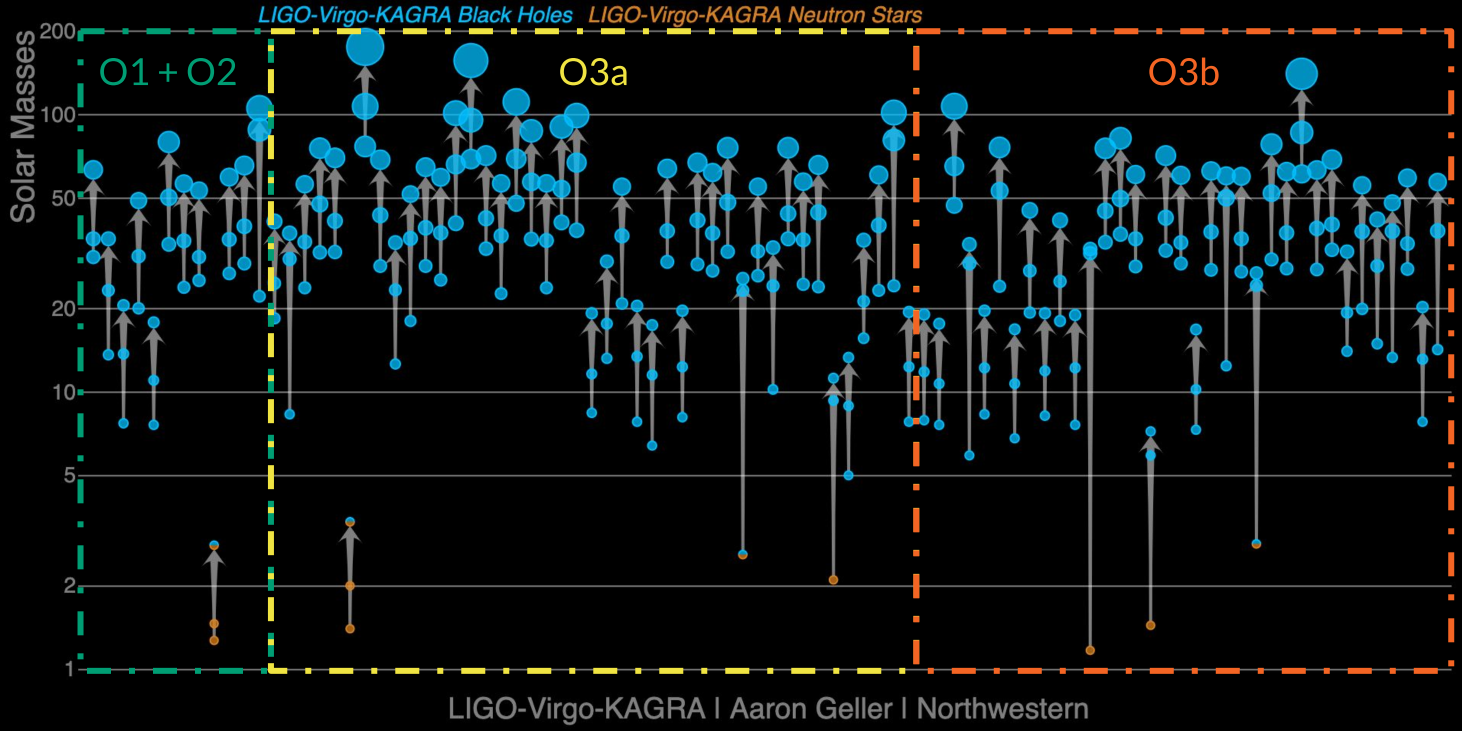

A Growing Catalog : GWTC-3

GWTC-3 adds **35** events with **more than 50% probability** of an **astrophysical** source

Total number of events is now 90

We analyze the **67 events** with false alarm rate (FAR) below ¼ yr^{-1}

Most are binary black holes **(BBH)**

Some are neutron star - black hole binaries **(NSBH)**

Two are binary neutron stars **(BNS)**

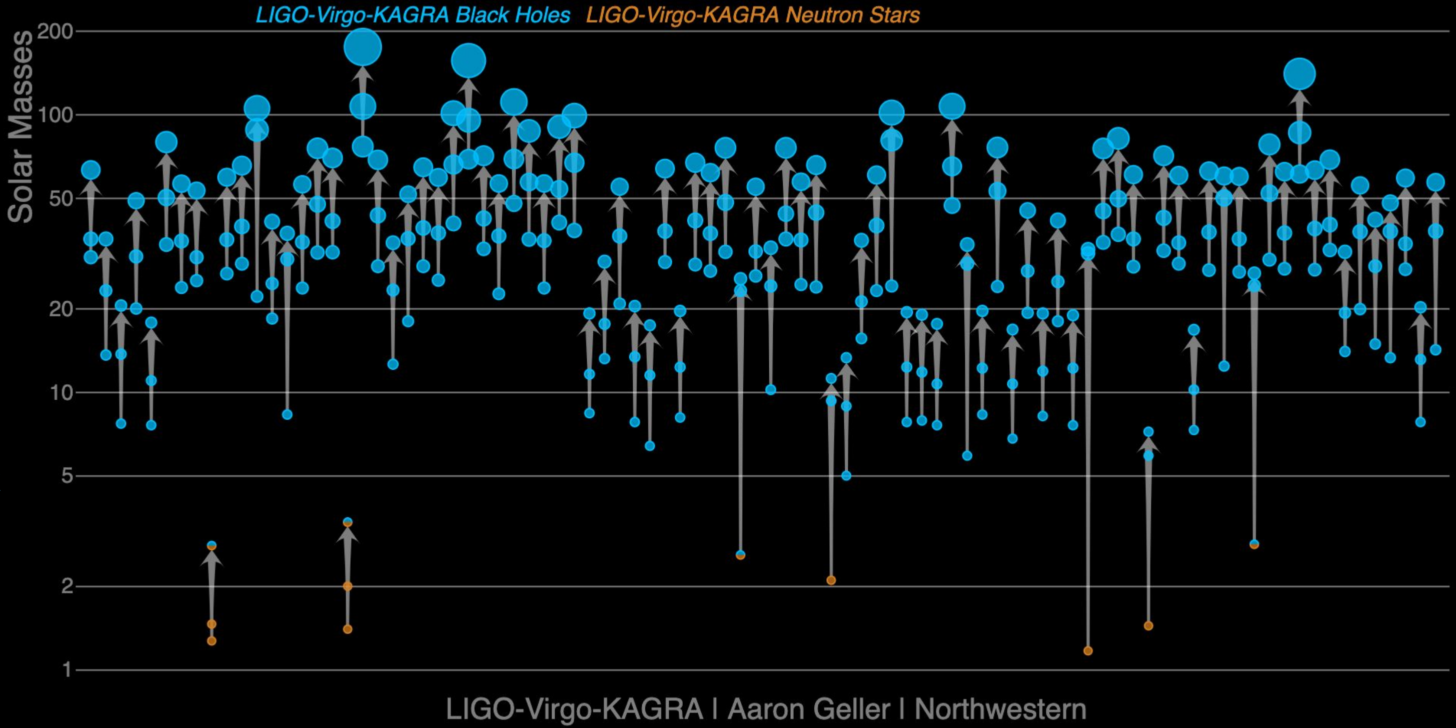

Population of GW Sources

- Population analysis to **understand individual events**

- Features found in the population shed light on the **astrophysical origins** of the systems we observe

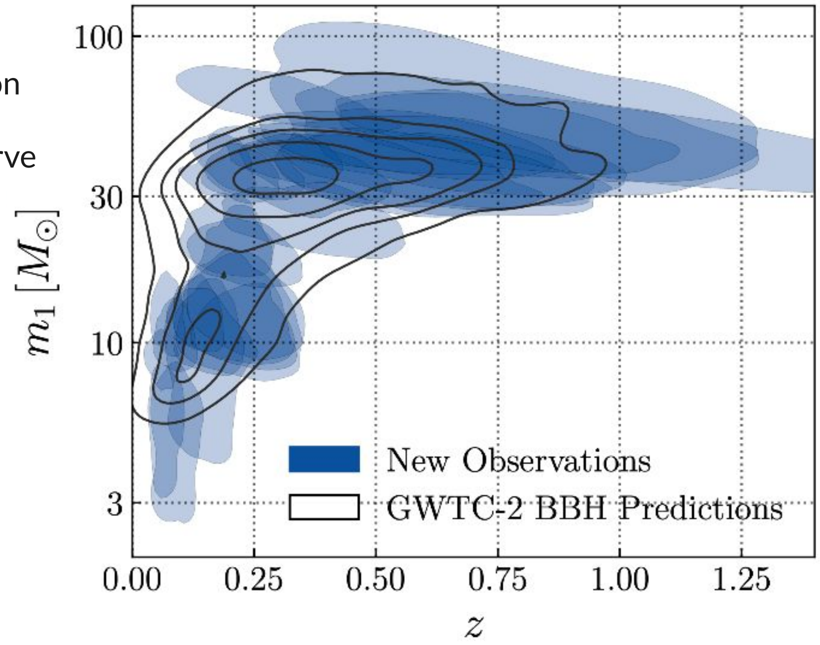

GWTC-2 population study: link

Methods and Inputs

- **67** events with **false alarm rate (FAR) below ¼ yr^{-1}**
- **masses**, **spins**, and **distances** of all these events inferred from the gravitational wave signal

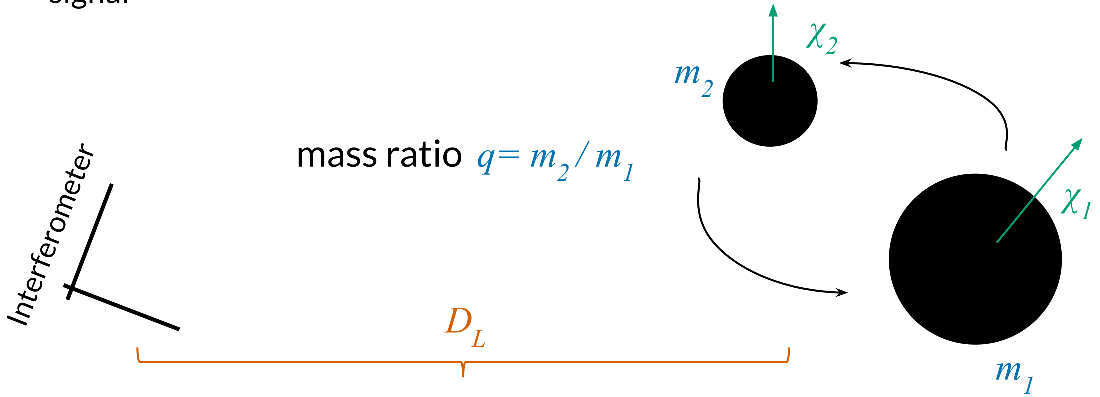

- Use a **hierarchical Bayesian analysis** to get an **astrophysical distribution of sources**
- Take **selection effects** into account
- **several** mass models, **3** spin models, and **one** distance model for the **astrophysical population** of sources

Details of how we infer the masses, spins, and other source parameters are in [the catalog paper]

Sensitivity estimates for modeling selection effects are on [Zenodo]

Merger rates of all sources

Subpopulations

Lower Mass Gap

Introduction Inputs Methods → Full Spectrum of Mergers → BNS and NSBH → BBH Mass → BBH Redshift and Spin

Full Spectrum of Compact Objects

We are sensitive to two types of compact objects: **neutron stars** and **black holes**

Three types of mergers: **binary neutron star**, **binary black hole**, **neutron star - black hole**

Fundamental Questions:

- Which types of mergers are we seeing?
- How many are happening in the Universe?

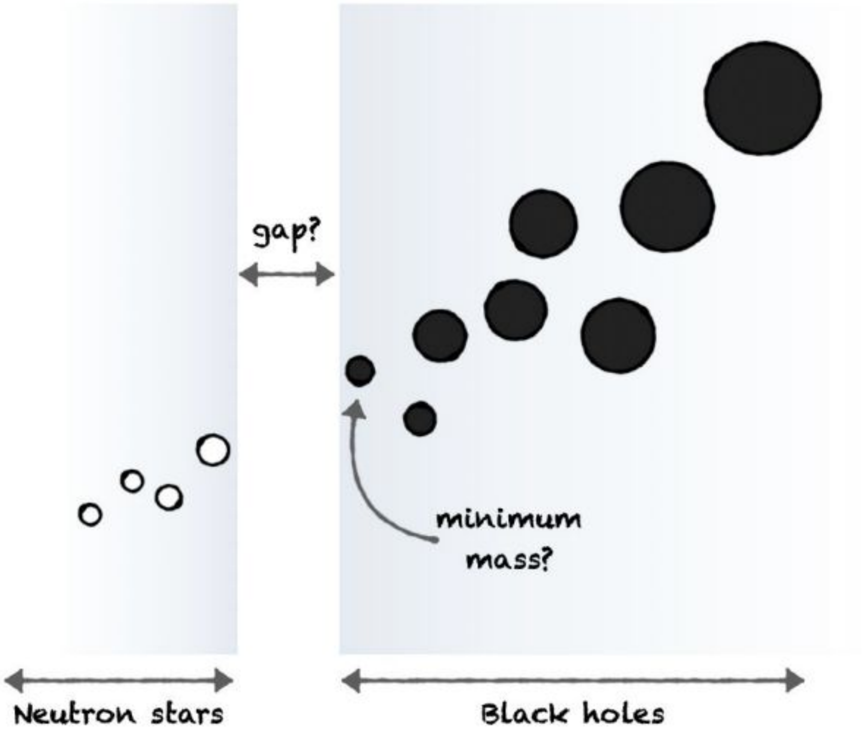

Full Spectrum of Compact Objects

- Models spanning the full spectrum of compact objects allow us to
  - Search for a **feature between neutron stars and black holes**
  - Find relative **rates** of mergers in different parts of the spectrum
  - Include **ambiguously classified events**

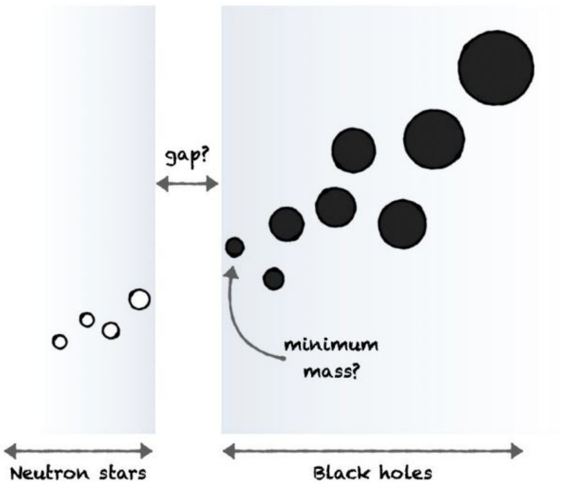

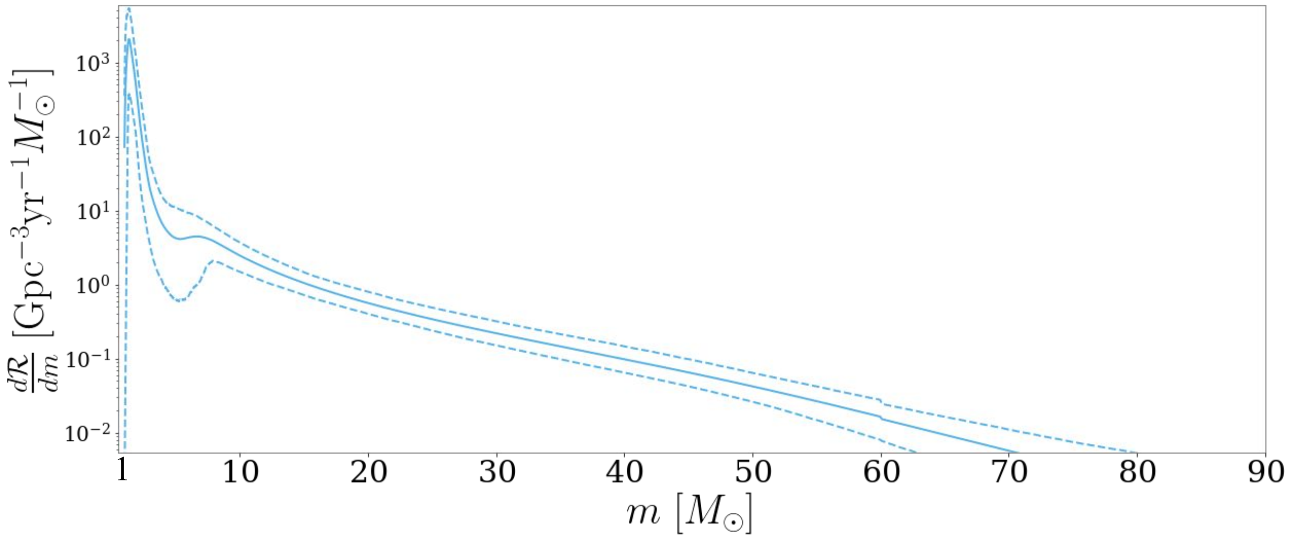

Features and Merger Rates

PDB: Power Law + Dip + Break

MS: Multi-Source

BGP: Binned Gaussian Process

- **Multiple models** consistent with same results

$$\mathcal{R}_{\text{total}} = 470^{+830}_{-300}\ \text{Gpc}^{-3}\text{yr}^{-1}$$

$$\mathcal{R}_{\text{BNS}} = 250^{+640}_{-200}\ \text{Gpc}^{-3}\text{yr}^{-1}$$

$$\mathcal{R}_{\text{NSBH}} = 170^{+150}_{-89}\ \text{Gpc}^{-3}\text{yr}^{-1}$$

$$\mathcal{R}_{\text{BBH}} = 22^{+9}_{-6}\ \text{Gpc}^{-3}\text{yr}^{-1}$$

- **Steep drop-off** in the merger rate after neutron star-like masses
- Potential but **yet-unresolved** upper edge of mass gap

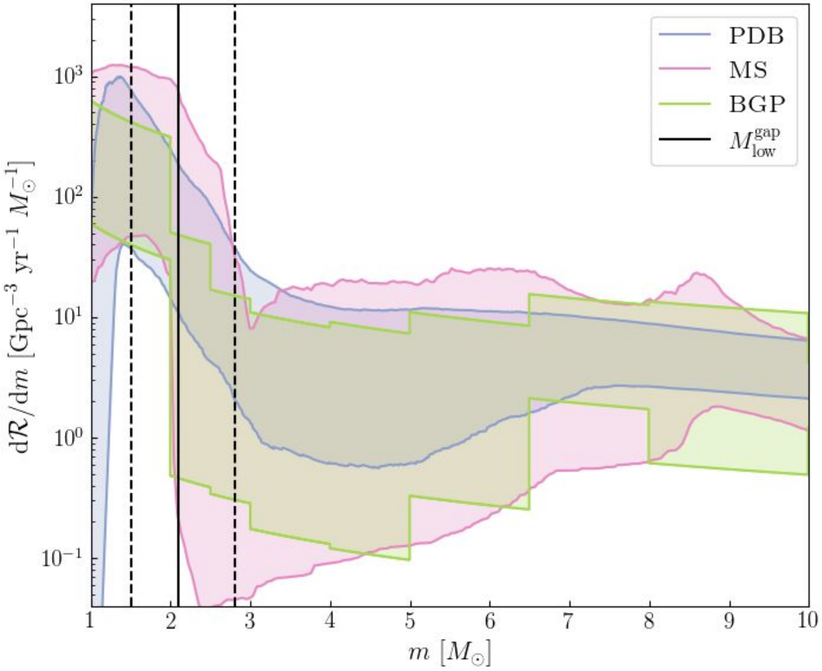

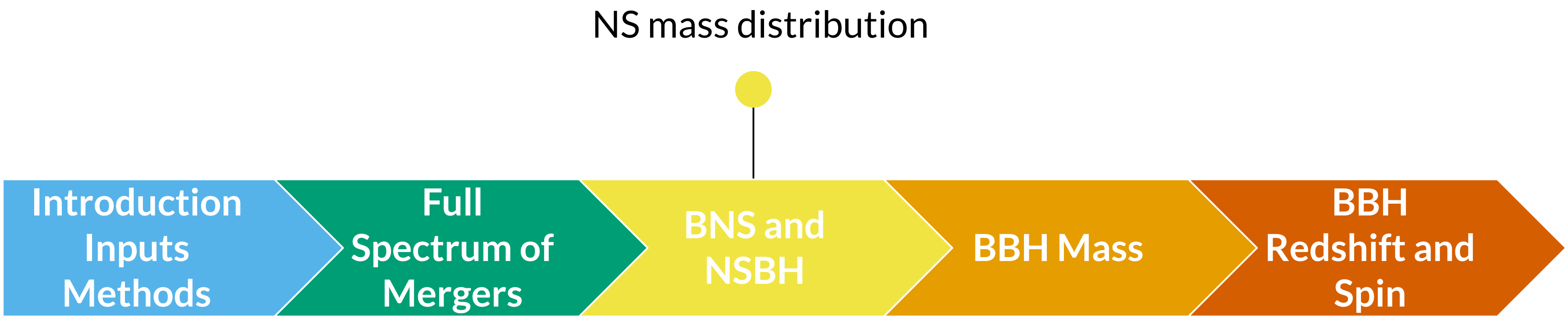
NS mass distribution
Introduction Inputs Methods
Full Spectrum of Mergers
BNS and NSBH
BBH Mass
BBH Redshift and Spin

Neutron star candidates

Five events with a low-mass component ($m < 3\,M_\odot$)

We infer the distribution of NS masses in merging compact binaries from a subset of these events

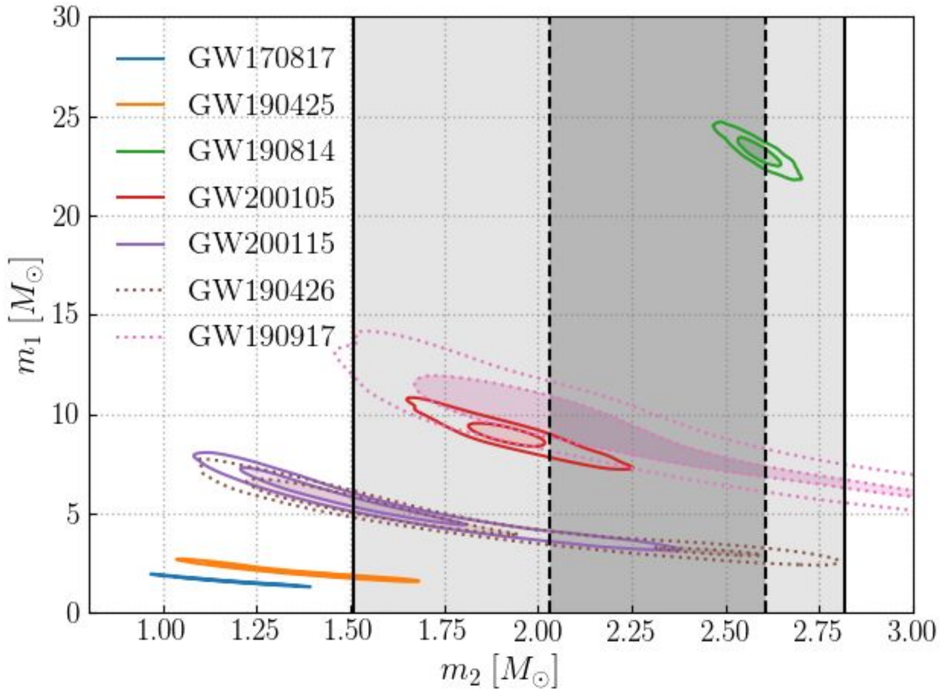

Classifying objects as neutron stars

- Treat low-mass components as NSs if $P(m \leq M_{TOV}) > 50\%$
- Obtain same classifications relative to M_{low}^{gap} instead of M_{TOV}

M_{TOV} is the non-rotating maximum NS mass estimated from current NS equation of state knowledge

M_{low}^{gap} is the inferred lower edge of the mass gap between NSs and BHs

GW190814 is a BBH according to this classification

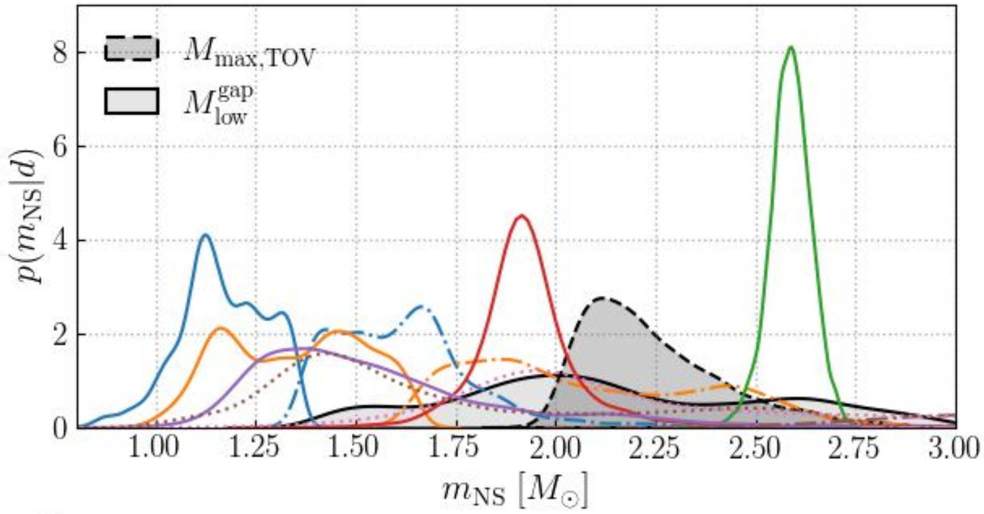

Six NSs in total

⇩

GW170817 x 2

GW190425 x 2

GW200105 x 1

GW200115 x 1

M_{TOV} from Legred *et al.* 2106.05313

Neutron star mass distribution

Recover broad mass distribution with more support for heavy NSs than Galactic population

Gaussian Peak model does not recover sharp peak at 1.35 $M_\odot$ observed in Galactic BNS population

Power model's exponent $\alpha = -2^{+5}_{-7}$ weakly constrained, but consistent with uniform distribution

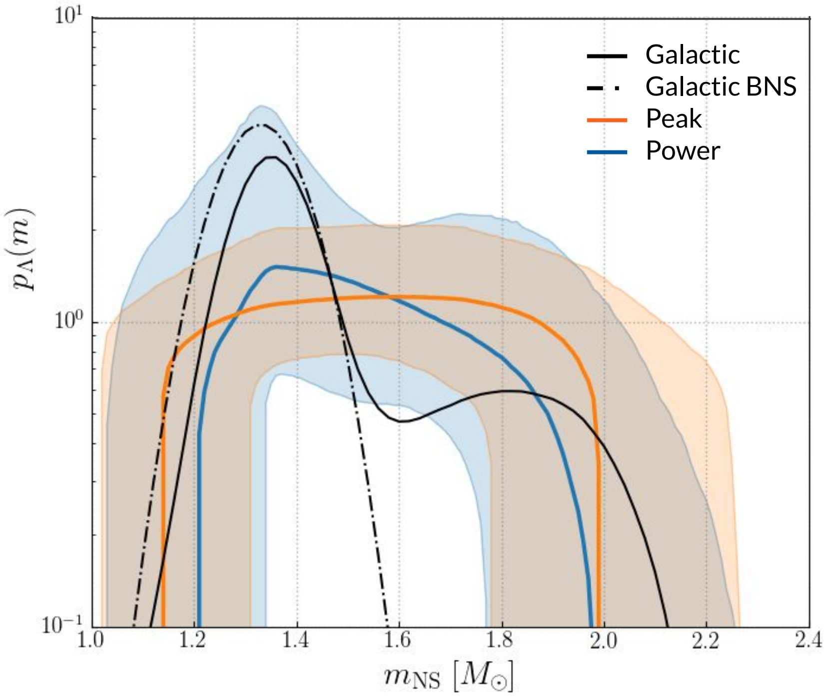

Difference relative to Galactic population could result from distinct formation channels, strong selection effects, or overlap of NS and BH mass distributions

Galactic fit from Farr & Chatziioannou 2005.00032, Galactic BNS fit from Ozel & Freire 1603.02698

Maximum neutron star mass

Maximum mass observed in the NS population is $m_{max} = 2.0^{+0.3}_{-0.2}\ M_\odot$

Observed maximum mass is consistent with $M_{TOV} = 2.2^{+0.3}_{-0.2}\ M_\odot$ from the equation of state

Also consistent with observed $m_{max} = 2.2^{+0.8}_{-0.2}\ M_\odot$ for Galactic pulsars

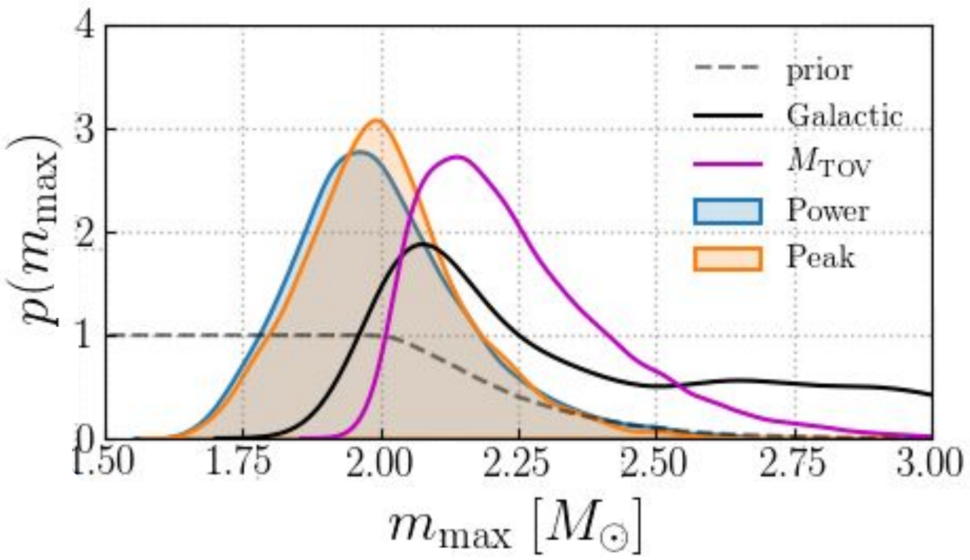

M_{TOV} from Legred *et al.* 2106.05313, Galactic m_{max} from Farr & Chatziioannou 2005.00032

Binary properties (I)

Introduction Inputs Methods

Full Spectrum of Mergers

BNS and NSBH

BBH Mass

BBH Redshift and Spin

Mass distribution

Results from our coarse grained model consistent between GWTC-2 and GWTC-3.

A higher fraction of low mass and unequal mass binaries observed in GWTC-3.

Steeper decline at lower masses and a broader mass ratio distribution

PowerLaw + Peak

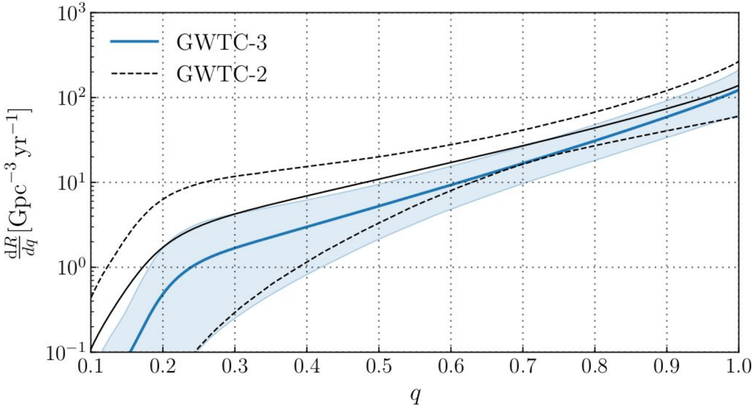

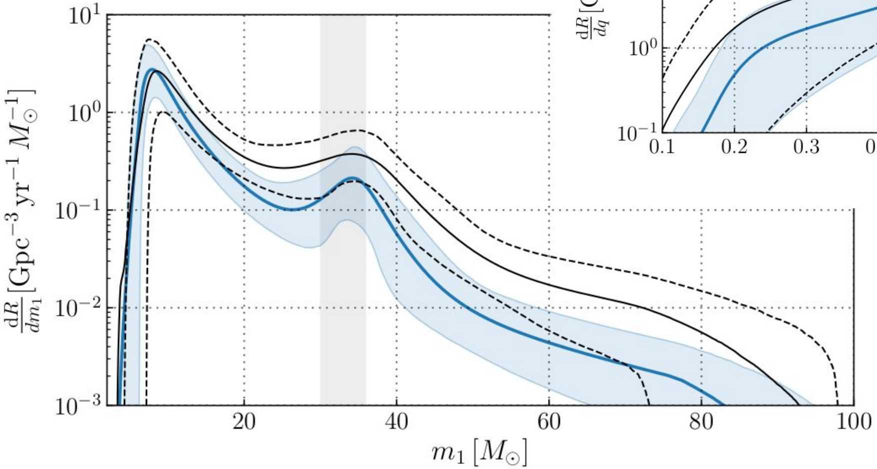

Mass distribution

Overdensity between 8$M_{\odot}$ and 10$M_{\odot}$, and around 26$M_{\odot}$.

One-eighth of the observations in the first overdensity.

Absence of mergers with chirp masses between 10$M_{\odot}$ and 12$M_{\odot}$.

A weaker feature present at around 14$M_{\odot}$

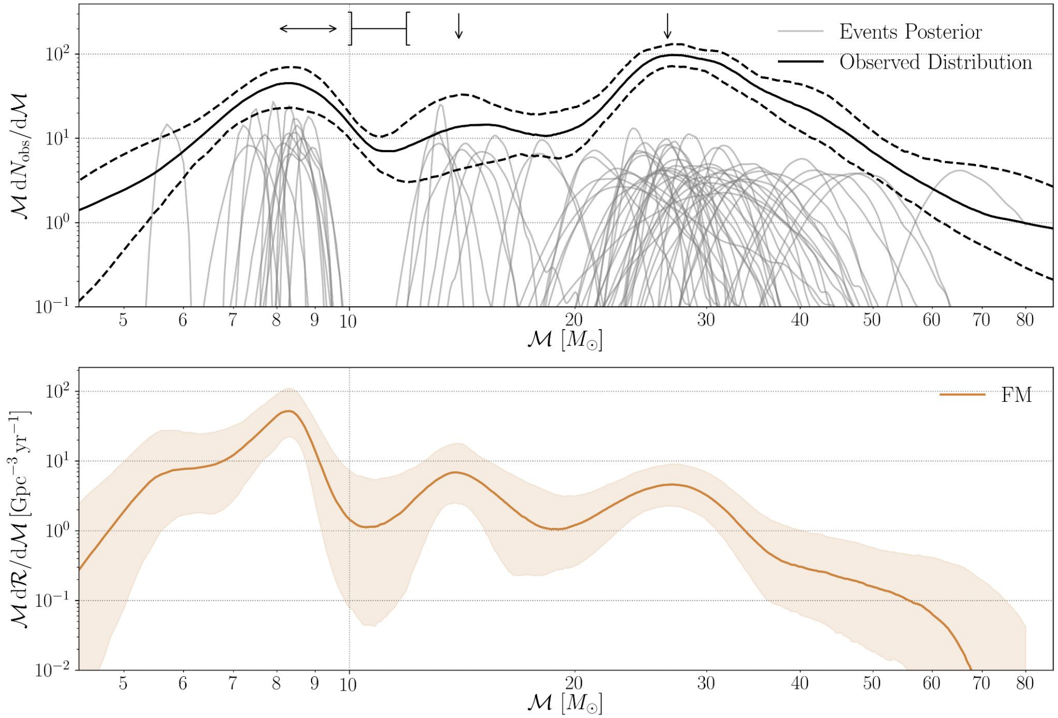

FM: Flexible Mixture

$$\mathcal{M} = (m_1 m_2)^{3/5}/(m_1 + m_2)^{1/5}$$

Mass distribution

Addition of more flexible models for the mass distribution.

Overdensity at 10M$_\odot$ and 35M$_\odot$ at a credibility greater than 99%.

Overdensity at 10M$_\odot$ contributes biggest fraction to the merger rate.

Overdensity at 35M$_\odot$ contributes biggest fraction to the observed mergers.

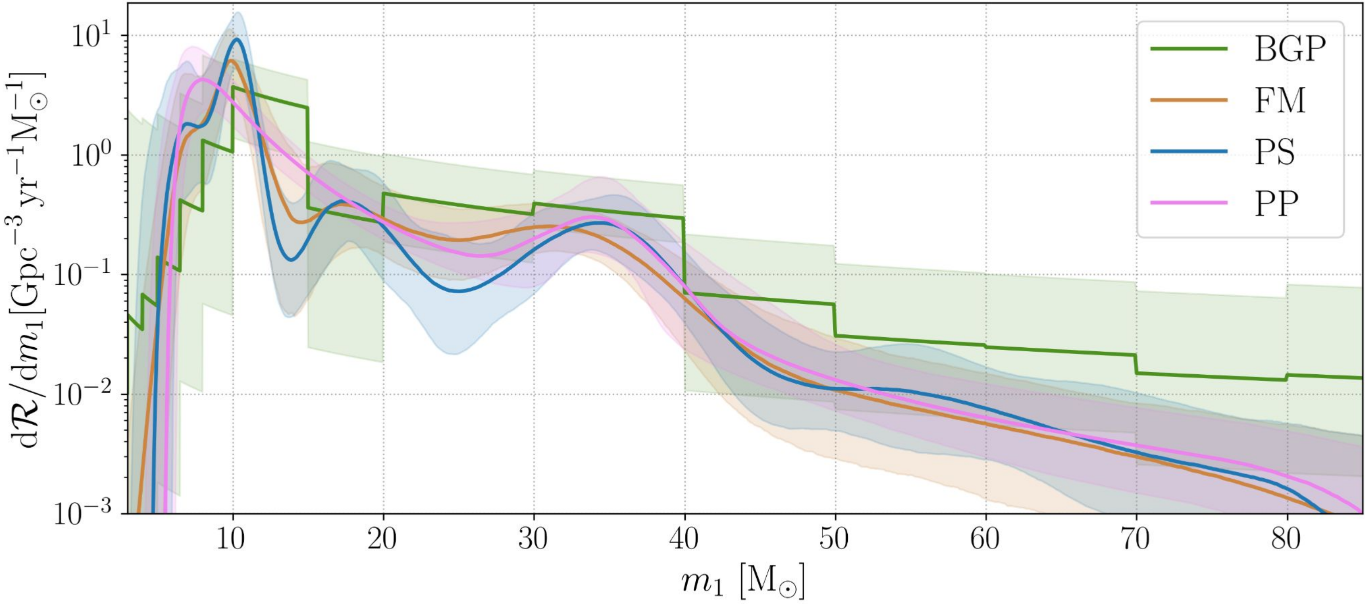

Mass distribution

Analysis dedicated to upper mass gap

No evidence for an upper mass gap

Mass gap higher than expected or heavier binaries formed in a way that avoids pair-instability.

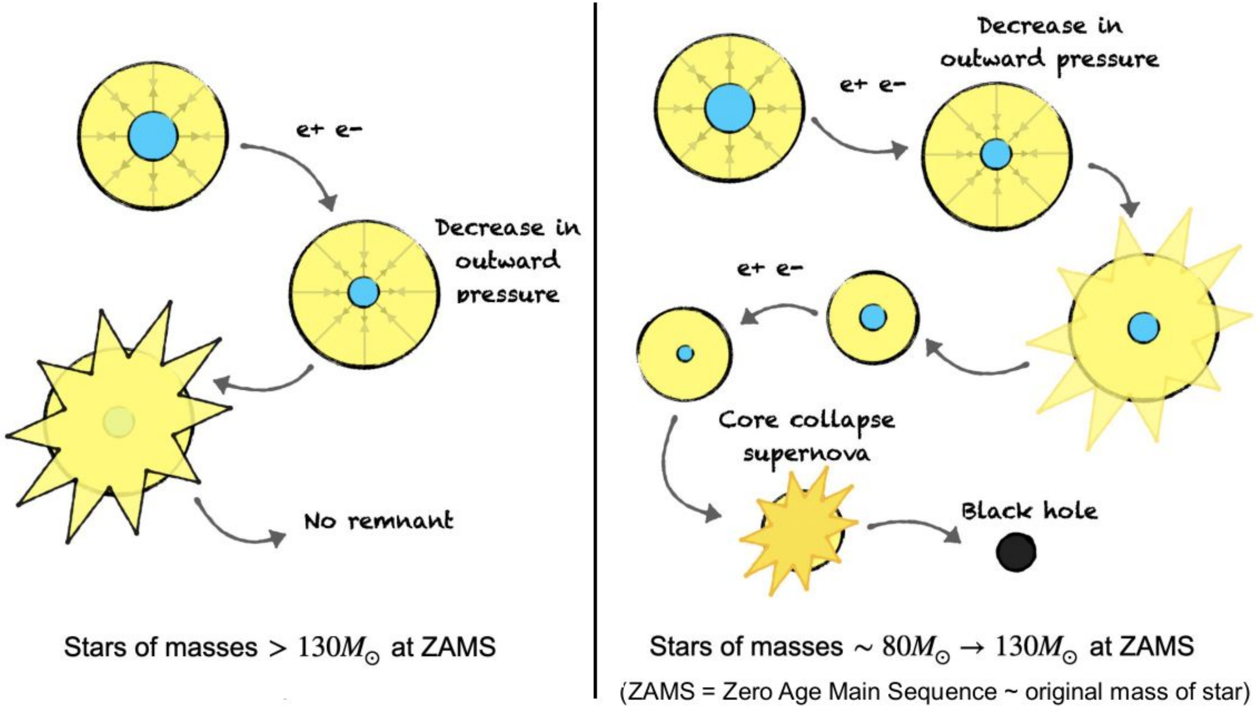

Mass distribution

GW190917 and GW190814 are outliers in binary black hole population.

Could suggest a separate subpopulation.

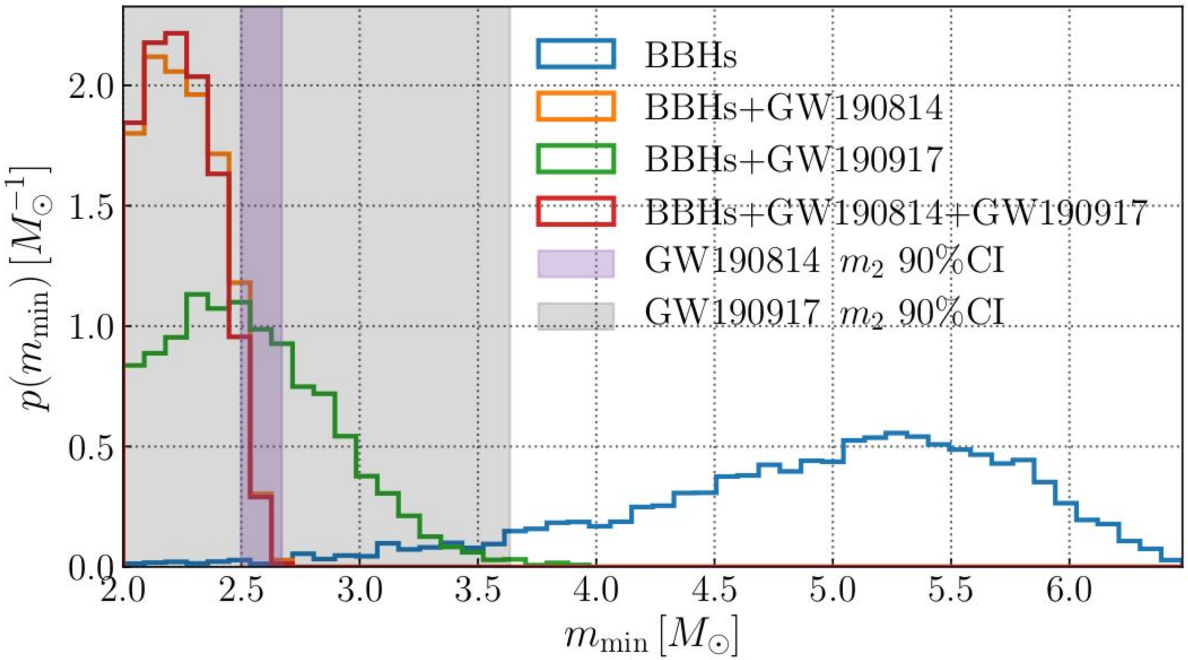

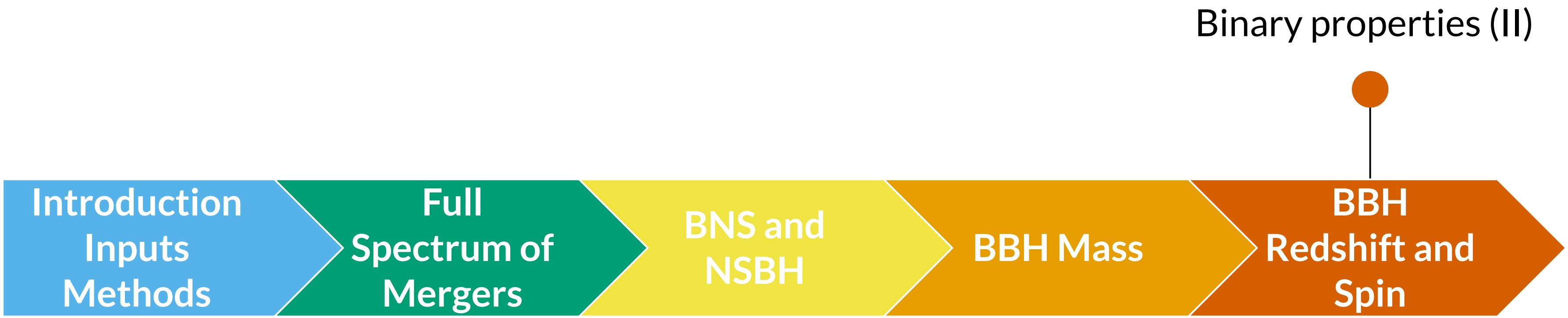
Binary properties (II)
Introduction Inputs Methods
Full Spectrum of Mergers
BNS and NSBH
BBH Mass
BBH Redshift and Spin

Redshift evolution

Analysis

Previous analyses were agnostic about evolution of the BBH merger rate

We now confidently conclude that the **merger rate rises into the past**

Result driven by new data and **improved estimates of search sensitivities**

No evidence that mass varies with redshift

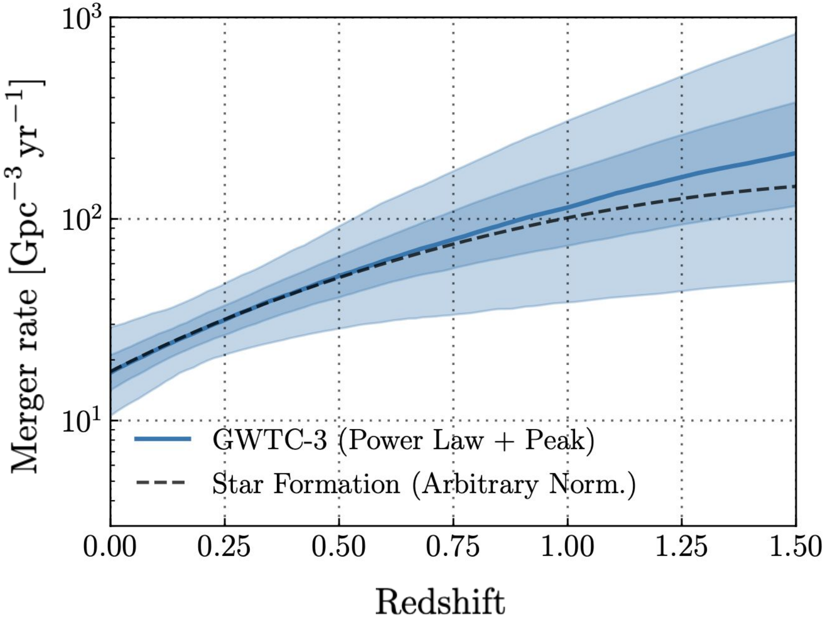

Spin distribution

Background

BBH spins explored via two complementary approaches:

Measurement of component **spin magnitudes** and **tilts**

Measurement of **effective spin parameters**:

$\chi_{\text{eff}} \approx$ average spin parallel to $\boldsymbol{L}$

$\chi_{\text{p}} \approx$ dominant spin perpendicular to $\boldsymbol{L}$

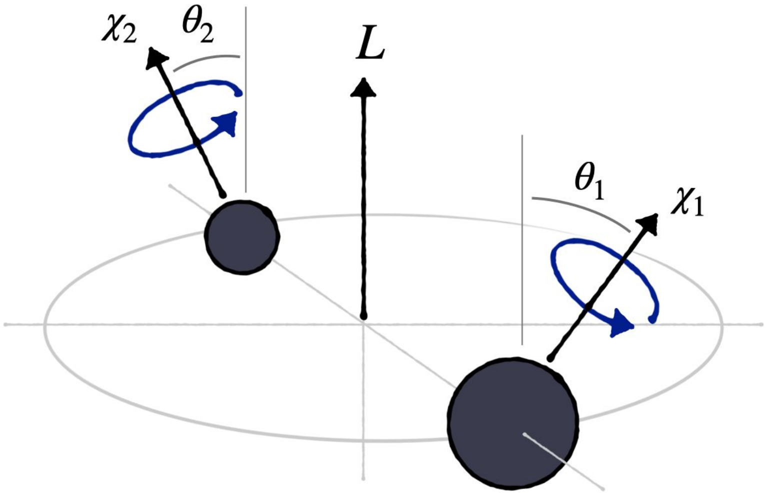

Spin distribution

Background

BBH spin orientations probe binary formation

Isolated field binaries: preferentially aligned spins

Dynamical assembly in clusters: isotropically aligned spins

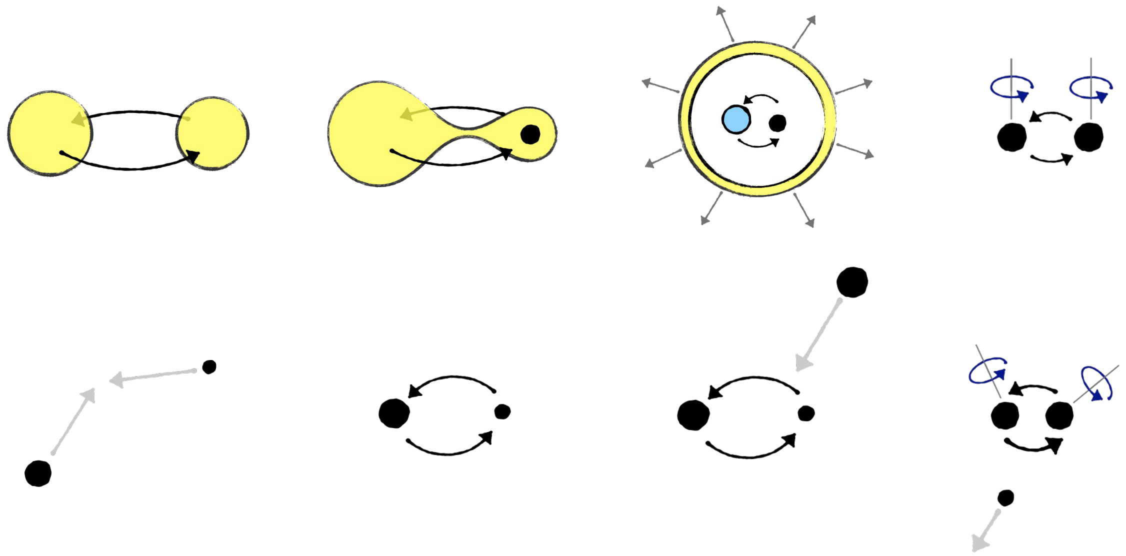

e.g. Mandel & Farmer 1806.05820

Spin distribution

Analysis

Spin magnitudes due to non-zero natal spins, or spin-up via binary tides & mass transfer?

Despite misalignment, spin orientations are not isotropic; challenge to purely-dynamical origin

Effective spins reveal non-vanishing χ_p and asymmetric χ_eff distributions

Ask us about this!

Spin magnitudes generally small but non-vanishing.

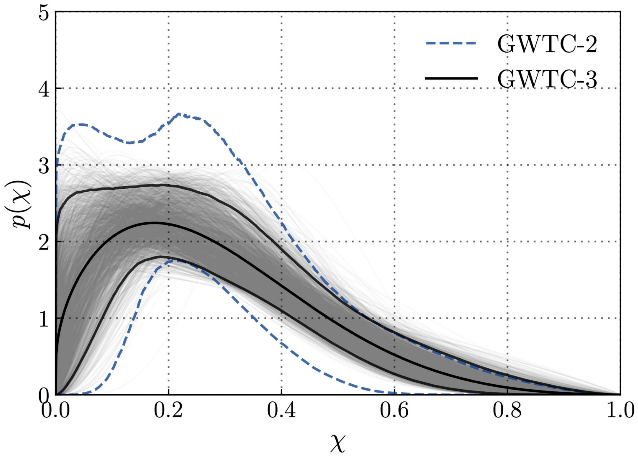

Significant spin-orbit misalignment

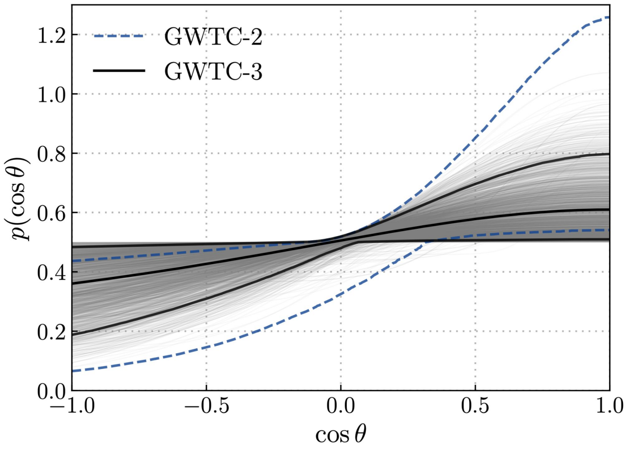

Correlations between spin and mass ratio

Analysis

Allow mean and standard deviation of $\chi_{\rm eff}$ to depend linearly on mass ratio q

On average, BBHs with more unequal masses have larger effective spins

Could signify preferentially larger or more aligned spins with unequal mass ratios

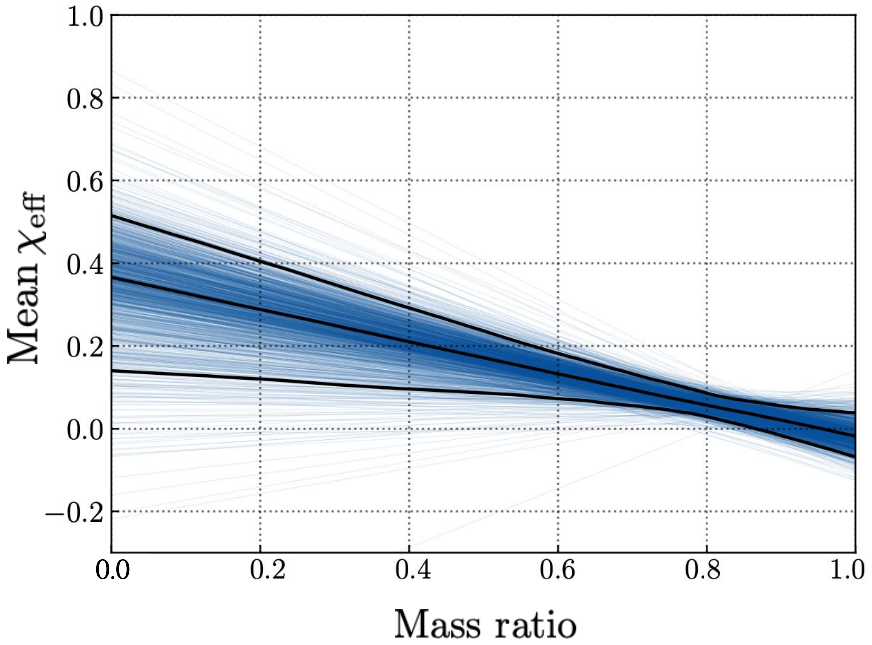

Callister *et al.* 2106.00521

Correlations between spin and mass

Analysis

A relationship between BH spins and masses might signify e.g. repeated “hierarchical” mergers

Sought to identify mass & spin correlations using the **Flexible Mixtures** approach

No evidence for a mass-dependent spin distribution

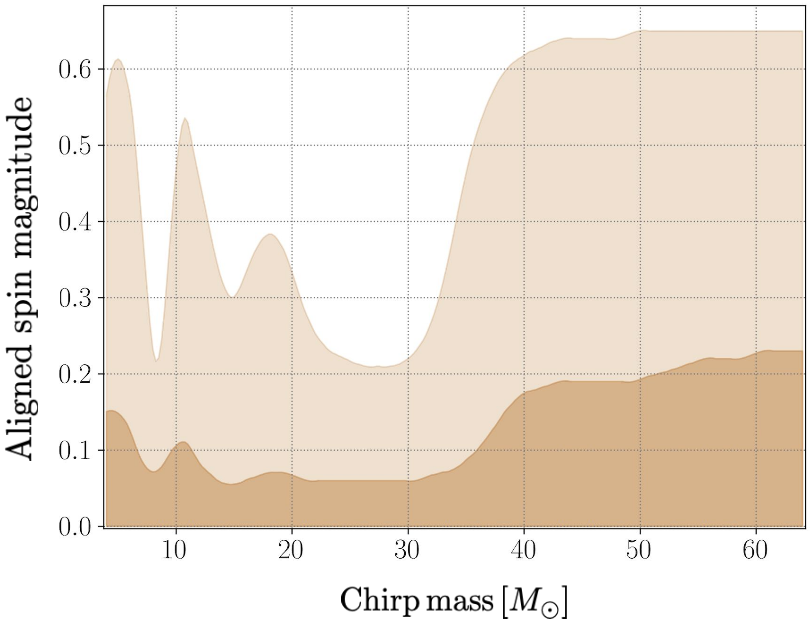

Summary

What we've learned

Look out for:

O4 observing run in December 2022

Upcoming webinar: Testing general relativity with GWTC-3 (20 Jan)

Neutron stars

Maximum mass consistent with TOV expectation

Systematically broader mass distribution than Galactic population

NS-BH binaries

Improved NS-BH rate estimates

BH-BH binaries

Global maximum at 10 $M_\odot$

Overdensity at 35 $M_\odot$

Merger rate increases with redshift

Misaligned spins

Correlations between spin and mass ratios

All sources

First self-consistent measurement of the merger rate across all masses

Data release

Data

Data products include full analyses used in paper

Notebooks and example **scripts** included with data products

Gravitational Wave Open Data Workshops provide more resources to understand data analysis

Data products

Analysis results available from www.gw-openscience.org/GWTC-3/ at https://doi.org/10.5281/zenodo.5650061

- Full posteriors for all analyses
- Python tutorials
- Search sensitivity (O3, and O1+O2+O3)
- Data for all tables
- Data behind the figures (soon: all figure generation scripts)

This material is based upon work supported by NSF's LIGO Laboratory which is a major facility fully funded by the National Science Foundation. The authors also gratefully acknowledge the support of the Science and Technology Facilities Council (STFC) of the United Kingdom, the Max-Planck-Society (MPS), and the State of Niedersachsen/Germany for support of the construction of Advanced LIGO and construction and operation of the GEO 600 detector. Additional support for Advanced LIGO was provided by the Australian Research Council. The authors gratefully acknowledge the Italian Istituto Nazionale di Fisica Nucleare (INFN), the French Centre National de la Recherche Scientifique (CNRS) and the Netherlands Organization for Scientific Research, for the construction and operation of the Virgo detector and the creation and support of the EGO consortium. The authors also gratefully acknowledge research support from these agencies as well as by the Council of Scientific and Industrial Research of India, the Department of Science and Technology, India, the Science & Engineering Research Board (SERB), India, the Ministry of Human Resource Development, India, the Spanish Agencia Estatal de Investigación, the Vicepresidència i Conselleria d'Innovació, Recerca i Turisme and the Conselleria d'Educació i Universitat del Govern de les Illes Balears, the Conselleria d'Innovació, Universitats, Ciència i Societat Digital de la Generalitat Valenciana and the CERCA Programme Generalitat de Catalunya, Spain, the National Science Centre of Poland and the Foundation for Polish Science (FNP), the Swiss National Science Foundation (SNSF), the Russian Foundation for Basic Research, the Russian Science Foundation, the European Commission, the European Regional Development Funds (ERDF), the Royal Society, the Scottish Funding Council, the Scottish Universities Physics Alliance, the Hungarian Scientific Research Fund (OTKA), the French Lyon Institute of Origins (LIO), the Belgian Fonds de la Recherche Scientifique (FRS-FNRS), Actions de Recherche Concertées (ARC) and Fonds Wetenschappelijk Onderzoek – Vlaanderen (FWO), Belgium, the Paris Île-de-France Region, the National Research, Development and Innovation Office Hungary (NKFIH), the National Research Foundation of Korea, the Natural Science and Engineering Research Council Canada, Canadian Foundation for Innovation (CFI), the Brazilian Ministry of Science, Technology, and Innovations, the International Center for Theoretical Physics South American Institute for Fundamental Research (ICTP-SAIFR), the Research Grants Council of Hong Kong, the National Natural Science Foundation of China (NSFC), the Leverhulme Trust, the Research Corporation, the Ministry of Science and Technology (MOST), Taiwan, the United States Department of Energy, and the Kavli Foundation. The authors gratefully acknowledge the support of the NSF, STFC, INFN and CNRS for provision of computational resources. Computing was performed on the OzSTAR Australian national facility at Swinburne University of Technology, which receives funding in part from the Astronomy National Collaborative Research Infrastructure Strategy (NCRIS) allocation provided by the Australian Government. We thankfully acknowledge the computer resources at MareNostrum and the technical support provided by Barcelona Supercomputing Center (RES-AECT-2021-2-0021). This work was supported by MEXT, JSPS Leading-edge Research Infrastructure Program, JSPS Grant-in- Aid for Specially Promoted Research 26000005, JSPS Grant-in-Aid for Scientific Research on Innovative Areas 2905: JP17H06358, JP17H06361 and JP17H06364, JSPS Core-to-Core Program A. Advanced Research Networks, JSPS Grant-in-Aid for Scientific Research (S) 17H06133, the joint research program of the Institute for Cosmic Ray Research, University of Tokyo, National Research Foundation (NRF) and Computing Infrastructure Project of KISTI-GSDC in Korea, Academia Sinica (AS), AS Grid Center (ASGC) and the Ministry of Science and Technology (MoST) in Taiwan under grants including AS-CDA-105-M06, Advanced Technology Center (ATC) of NAOJ, and Mechanical Engineering Center of KEK.

We would like to thank all of the essential workers who put their health at risk during the COVID-19 pandemic, without whom we would not have been able to complete this work.

Questions

Panelists

Fabio Antonini Cardiff University	Astro interpretation
Bruce Edelman University of Oregon	Black Hole Masses
Stephen Fairhurst Cardiff University	Additional events
Adrian Helmling-Cornell University of Oregon	Event selection
Jacob Golomb Caltech	Populations
Dan Wysocki UWM	Populations
Shanika Galaudage OzGrav/Monash University	Populations

Extra: GWTC-3

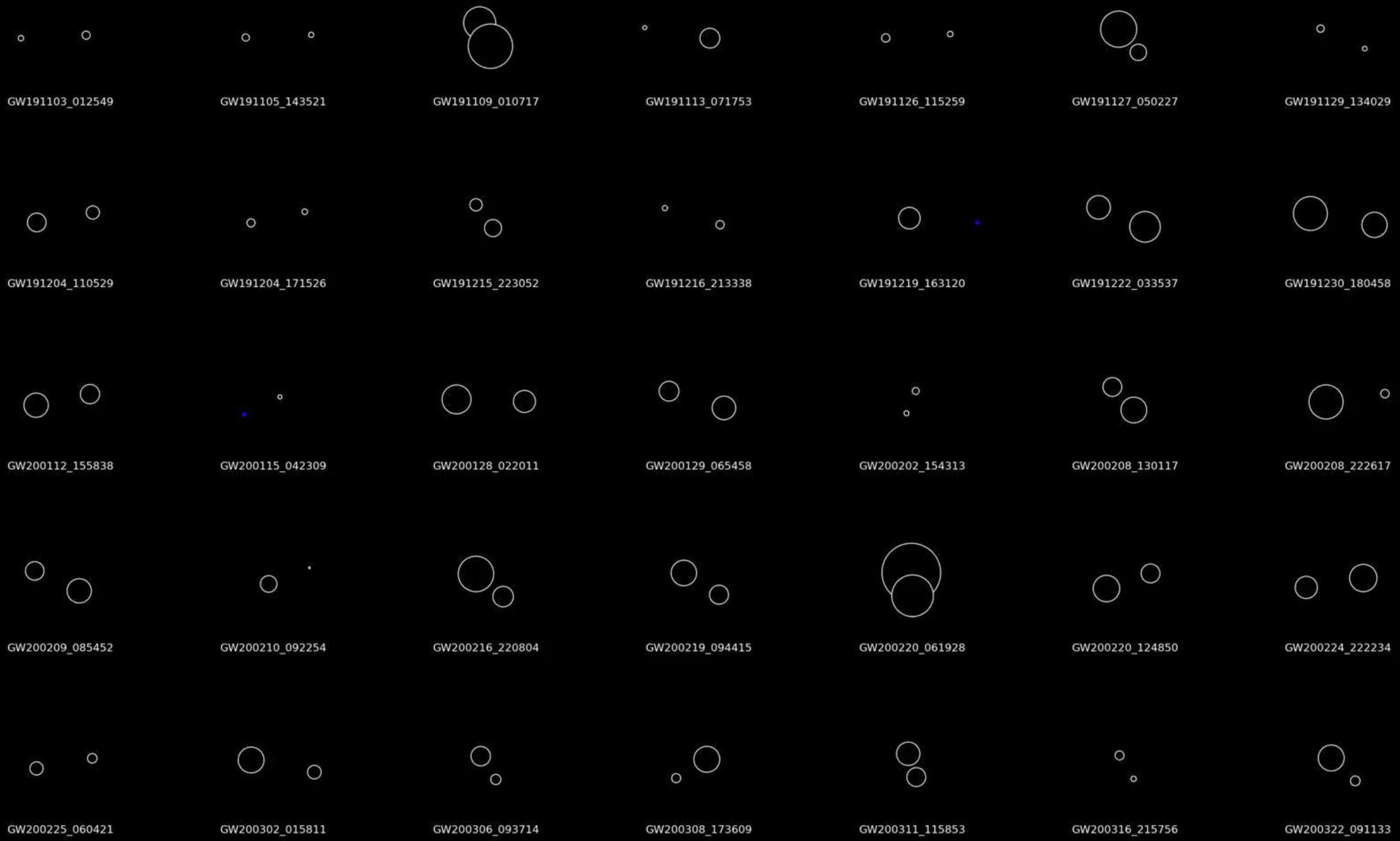

Zoheyr Doctor / CIERA / LIGO-Virgo Collaboration

Extra: Merger rate versus all mass

Details of models in these links:

[BGP](), [MSo](), [PDB]()

- Multiple methods to corroborate results

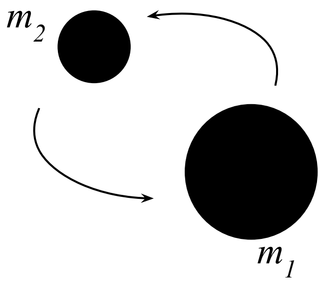

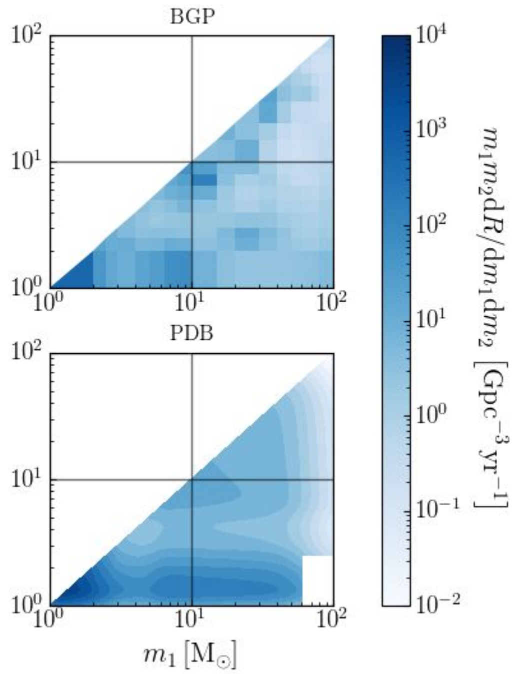

Takeaways so far

- **Growing catalog** gives us deeper insight into each event
- **Features** in the population can teach us **astrophysical lessons**
- We make the first self-consistent measurement of the **merger rate** of compact binaries across all masses
- Starting to resolve **transition between neutron stars and black holes**, which allows us to **classify** the two types of objects

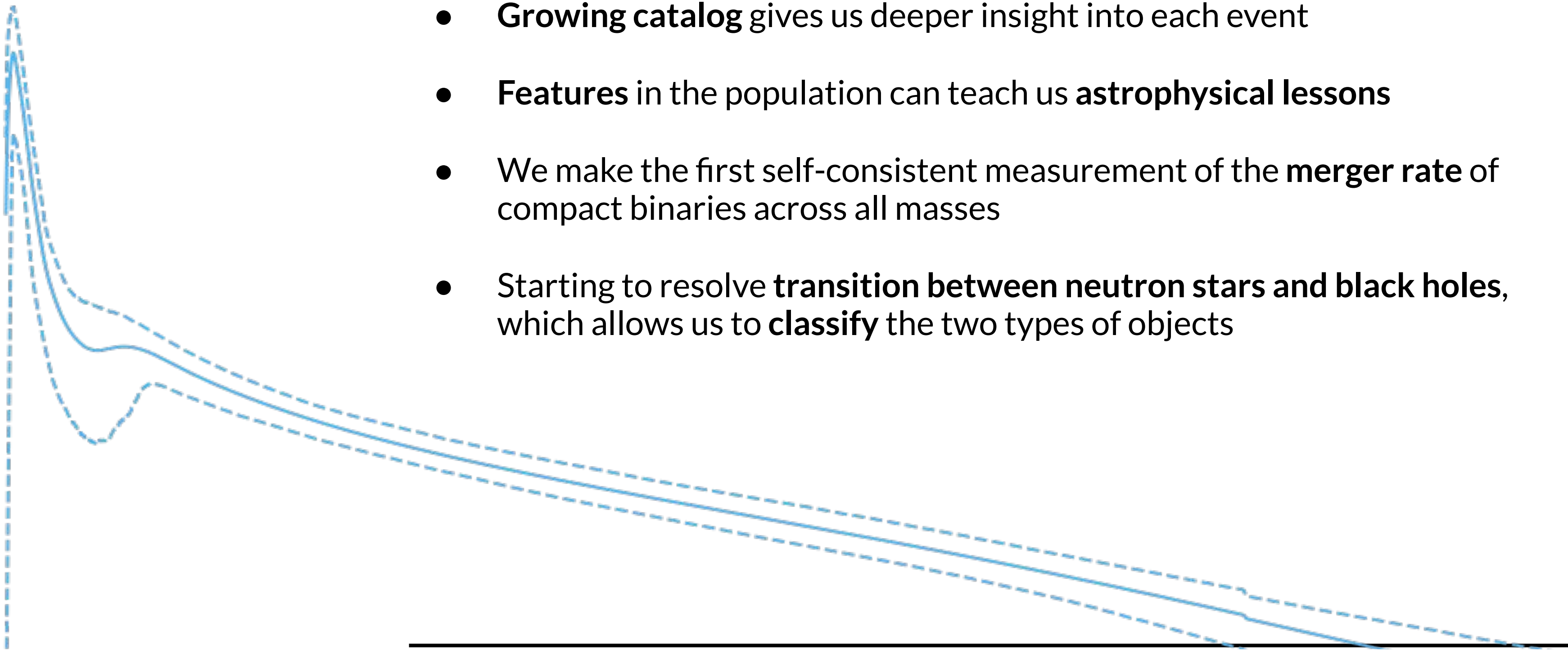

Source properties

Each signal we have detected so far has come from the merger of two compact objects- **neutron stars** and **black holes**

Using Bayesian inference, we analyse data to **infer source properties** like masses, spins, distance, and sky location

We use **waveform models** (see the GWTC-2.1 webinar)

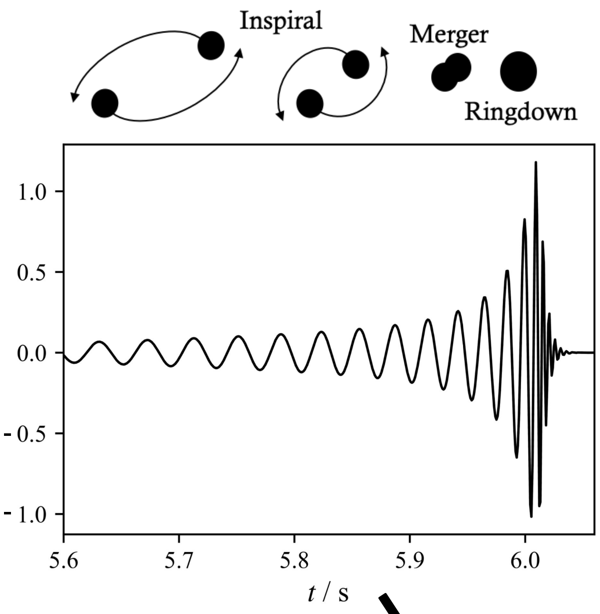

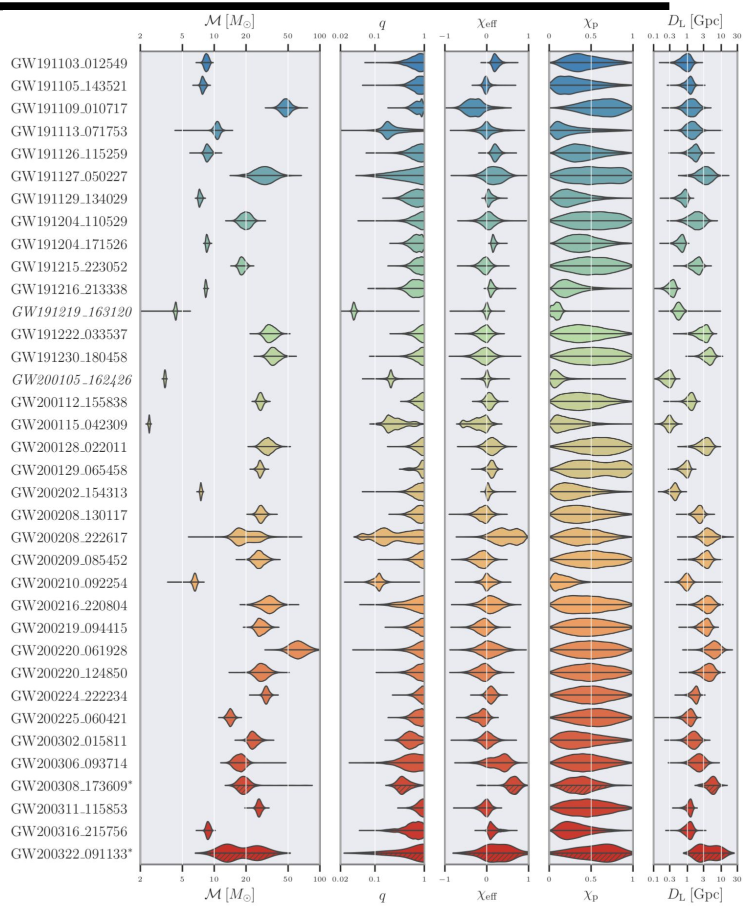

Extras: Effective spin parameters

Analysis

Effective spins fit as a **multivariate Gaussian**

Quite consistent with effective spin distributions implied by "**Default**" spin magnitude and tilt model

Asymmetric distribution of **effective inspiral spins**

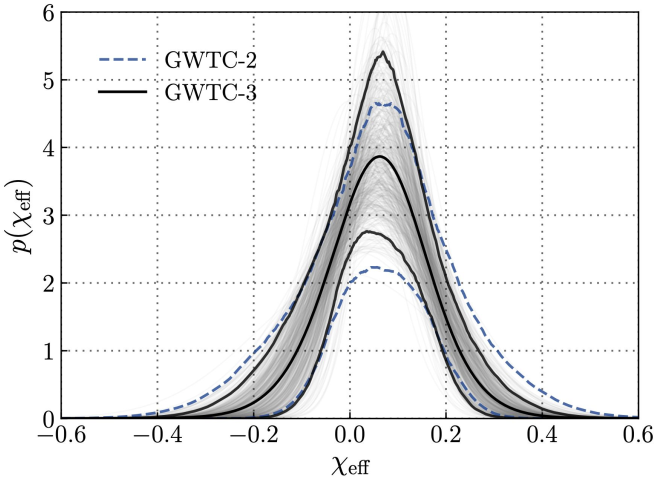

Non-vanishing distribution of **effective precessing spins**

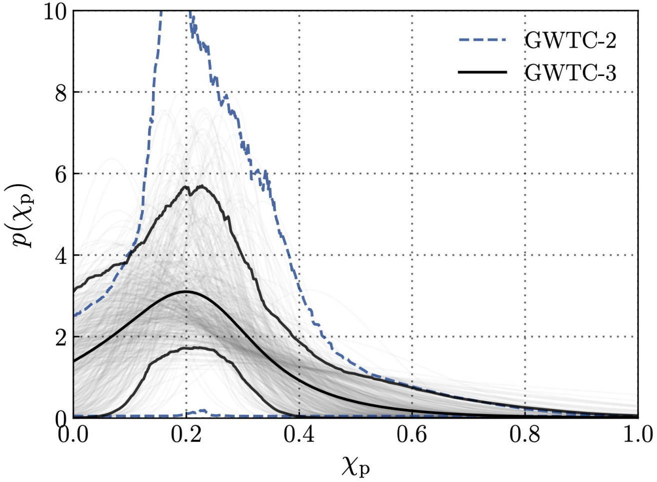

Extras: Negative effective spins?

Analysis

Negative effective spins would indicate spins misaligned by more than 90 degrees

Previously investigated by introducing a **variable lower truncation bound**

Updated analysis allows for additional overdensity at $\chi_{\rm eff} \approx 0$ to avoid possible systematics

Previous method

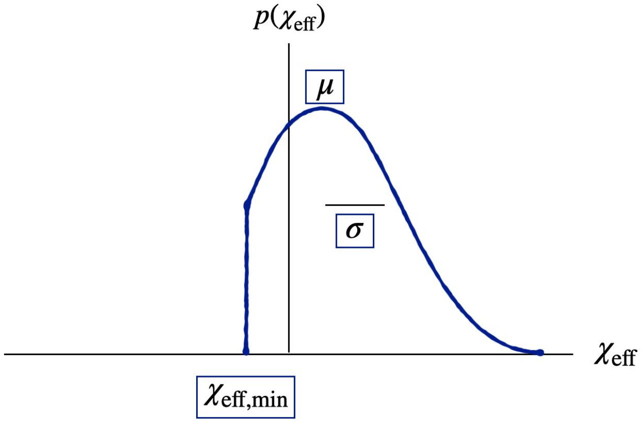

Updated method

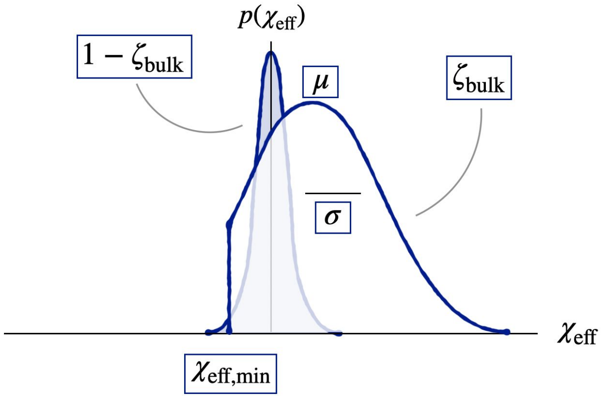

Extras: Negative effective spins?

Analysis

When assuming no overdensity, we find negative effective spins at 99.8% credibility

When allowing for overdensity, conclude that $\chi_{\rm eff,min} < 0$ at 88.4% credibility

Data do not require overdensity to exist

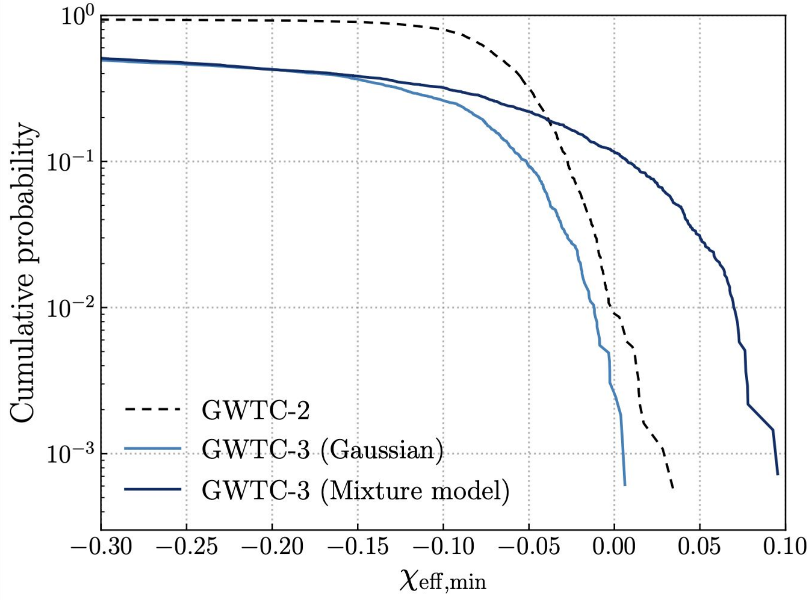

Extras: Other Events

Additional events not used in this analysis are broadly consistent with the observed population

Events from IAS searches: Venumadhav et al 1904.07214, Zackay et al 1910.09528

Events from OGC searches: Nitz et al 2105.09151

Events from GWTC-3 below threshold used in this analysis

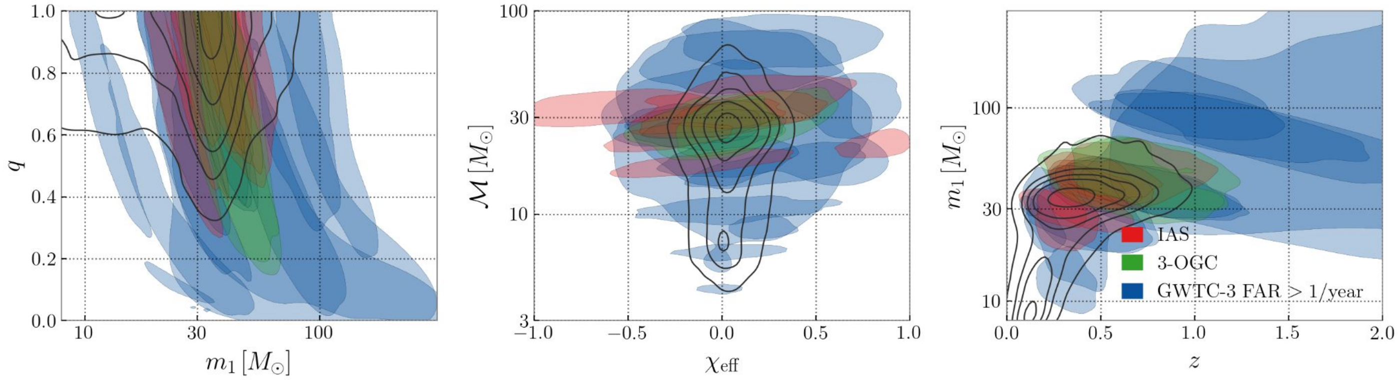

Modeled searches

Model signals as Compact Binary Coalescence (CBC)

Waveforms depend on intrinsic source parameters: component masses and the dimensionless component spins

$$M_c = \frac{(m_1 m_2)^{3/5}}{(m_1 + m_2)^{1/5}}$$

$$q = m_2 / m_1$$

$$\chi_{eff} = \frac{(m_1 \vec{\chi}_1 + m_2 \vec{\chi}_2) \cdot \hat{L}_N}{M}$$

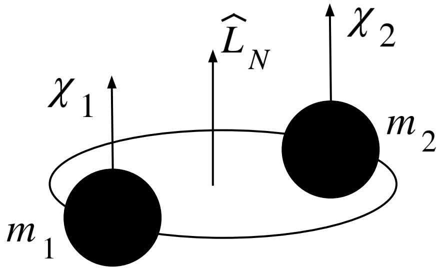

Template bank total masses
- MBTA: 2 - 200 Msun
- GstLAL: 2 - 758 Msun
- PyCBC: 2 - 500 Msun

Mass ratio
- MBTA:
- GstLAL: 0.02 - 1 (depends on parameter space region)
- PyCBC: ⅓ - 1

Spins
- MBTA: aligned spins up to 0.997
- GstLAL: anti- or aligned spins up to 0.999
- PyCBC: anti- or aligned spins up to 0.998

NSBH masses

Mass ratio q is **ratio** of **secondary** to **primary** mass:

$$q = \frac{m_2}{m_1}$$

Coloured contours in this plot are **confident** neutron star - black hole pairs

Grey contours in this plot are **ambiguous**, with secondary that may be a black hole or a neutron star

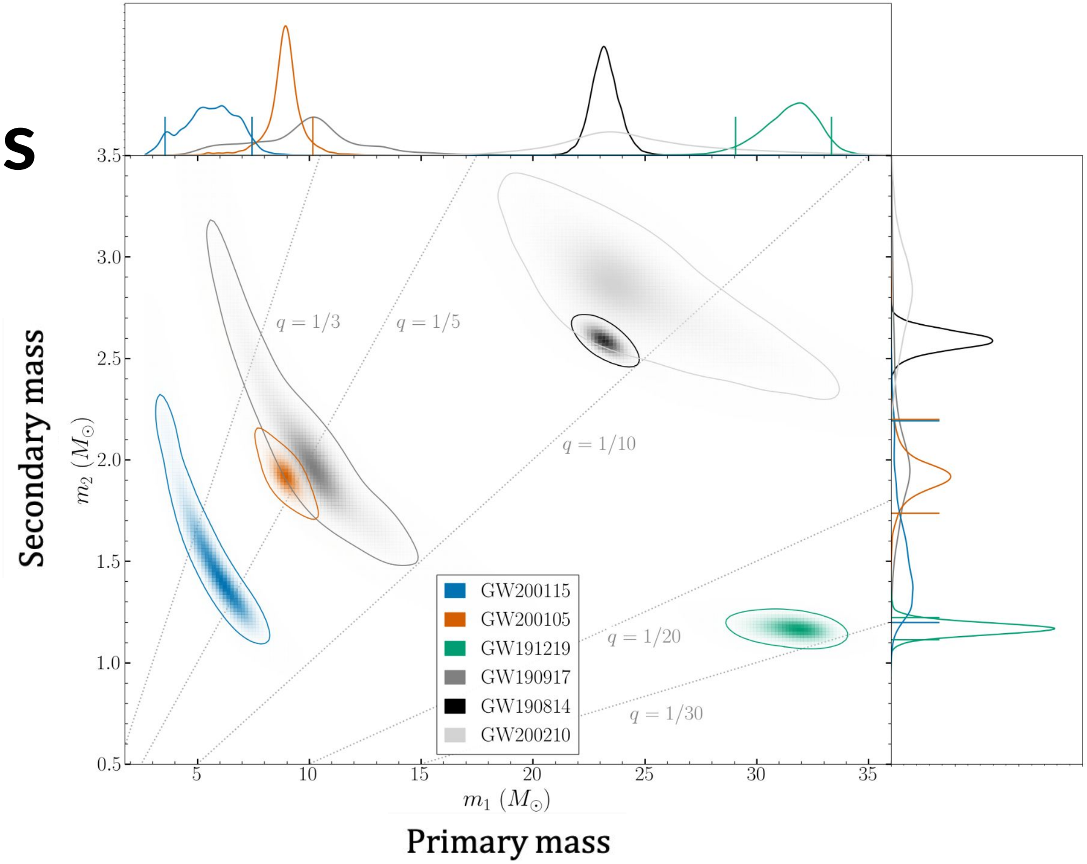

GW190814

GW190814's m_2 is an **outlier** relative to the population of BNS and NSBH secondaries

The GWTC-2 population study found that it is also an outlier from the BBH population

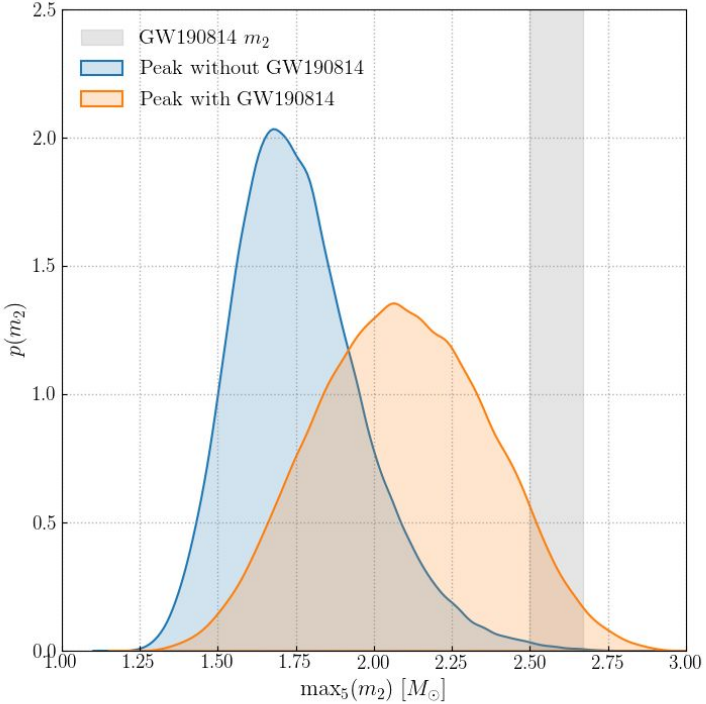

Peak model predicts largest m_2 observed after 2 BNSs and 3 NSBHs to be smaller than GW190814's m_2 99.9% of the time

Masses and spins

$$\mathcal{M} = \frac{(m_1 m_2)^{3/5}}{(m_1 + m_2)^{1/5}} \qquad \chi_{\mathrm{eff}} = \frac{m_1 \chi 1 + m_2 \chi 2}{m_1 + m_2}$$

Most effective inspiral spins **consistent with zero**

Some events with significant support for negative effective inspiral spins

More events have significant support for positive effective inspiral spins

Consistent with GWTC-2.1

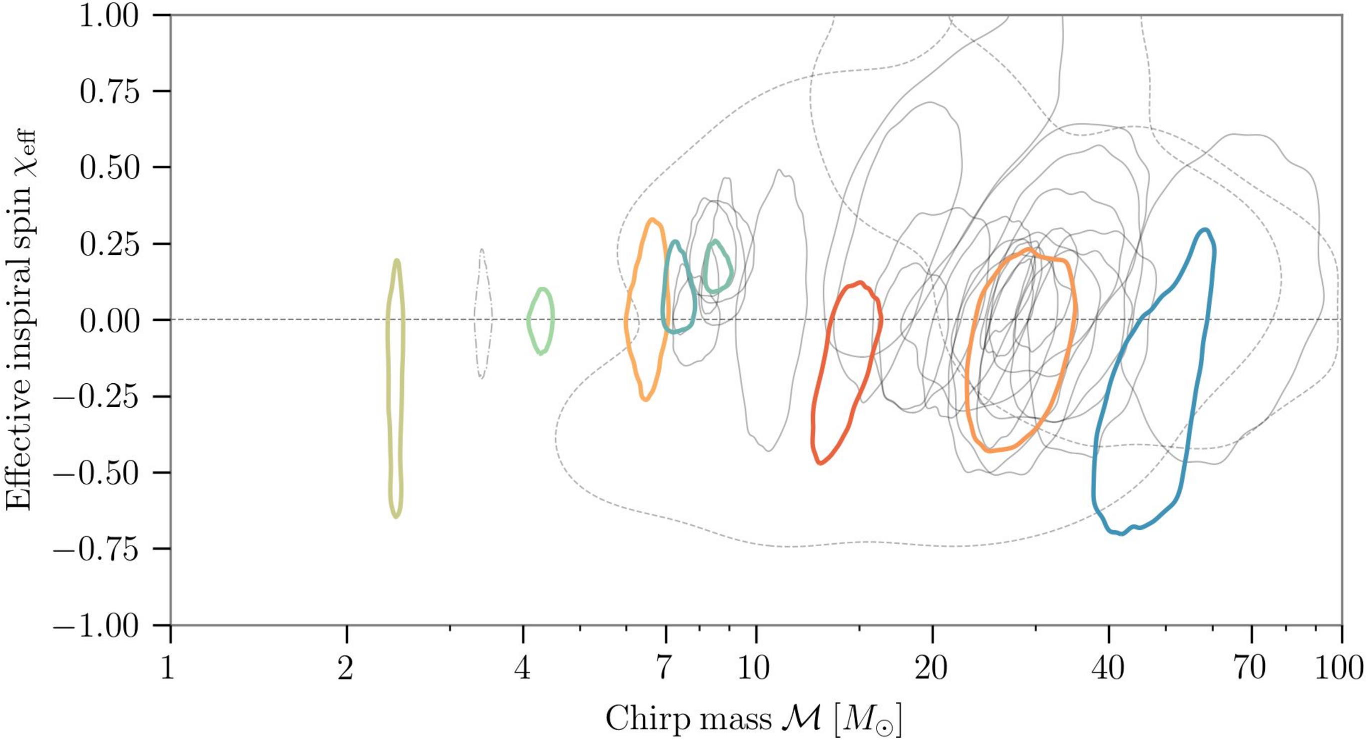

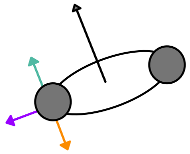

NSBH spins

Primary spin better measured as more important for dynamics

Spin components in the orbital plane better measured for more extreme mass ratios

Spins **approximately aligned** with orbital angular momentum expected for binaries formed in isolation

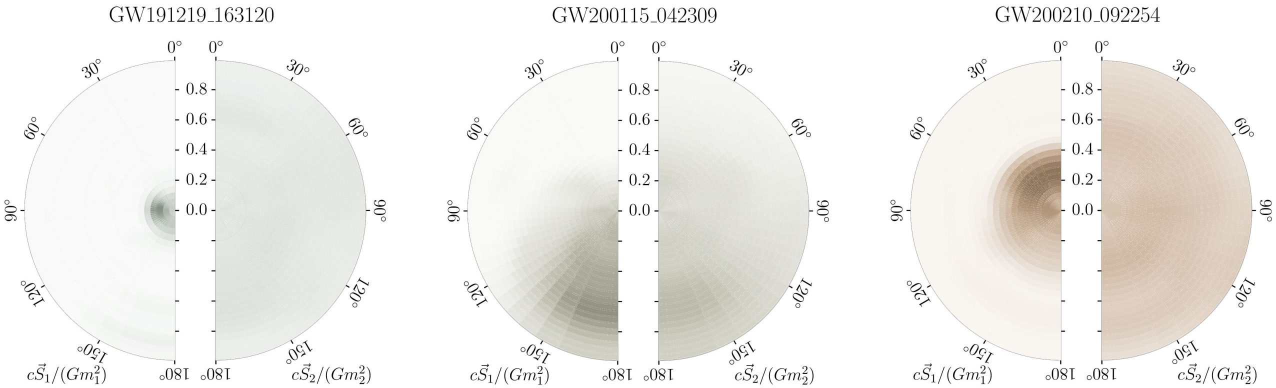

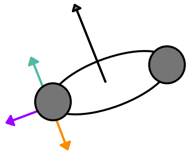

BBH spins: small / positive

Spins expected to be small if angular moment transfer is efficient in stars

Spins in X-ray binaries extend close to the Kerr limit of 1

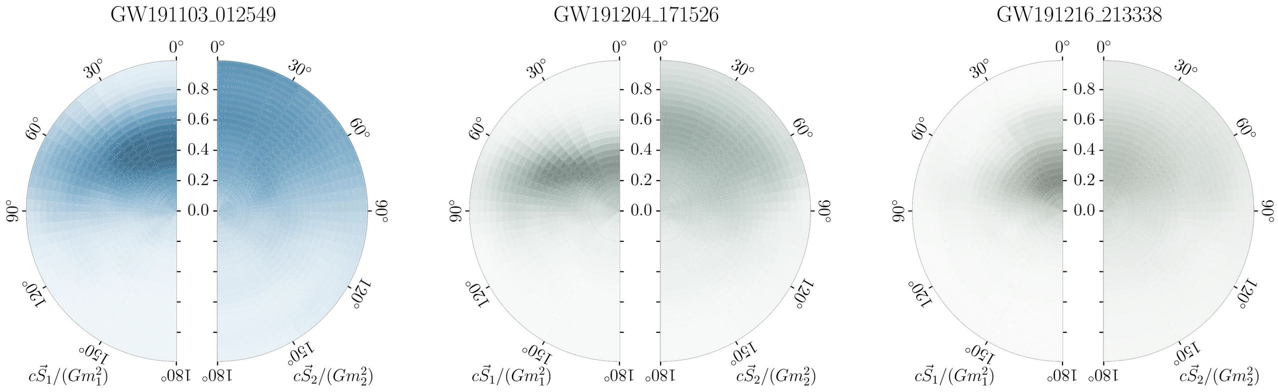

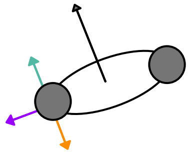

BBH spins: misaligned / negative

Misaligned spins expected for binaries formed dynamically

Equal-mass mergers produce spins around 0.7

GW200129 shows **best evidence for misaligned spins**

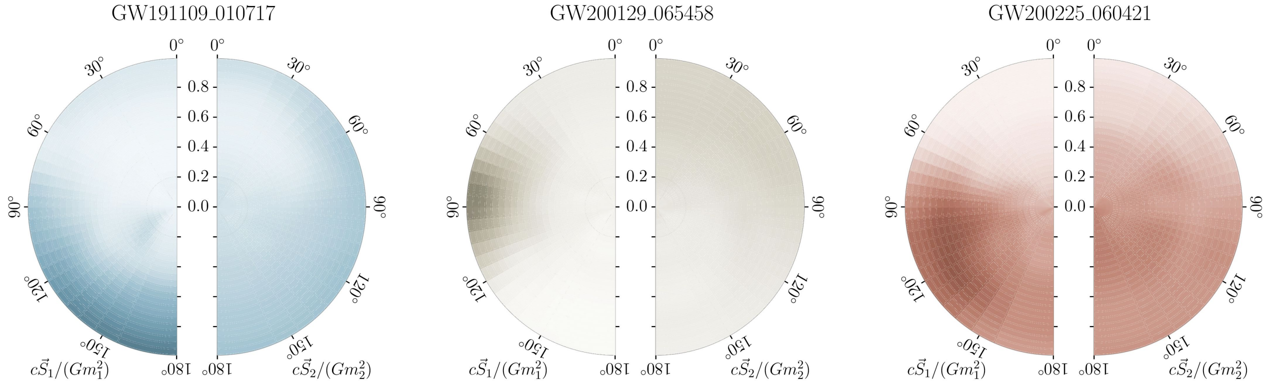

Highlighted events O3b catalog

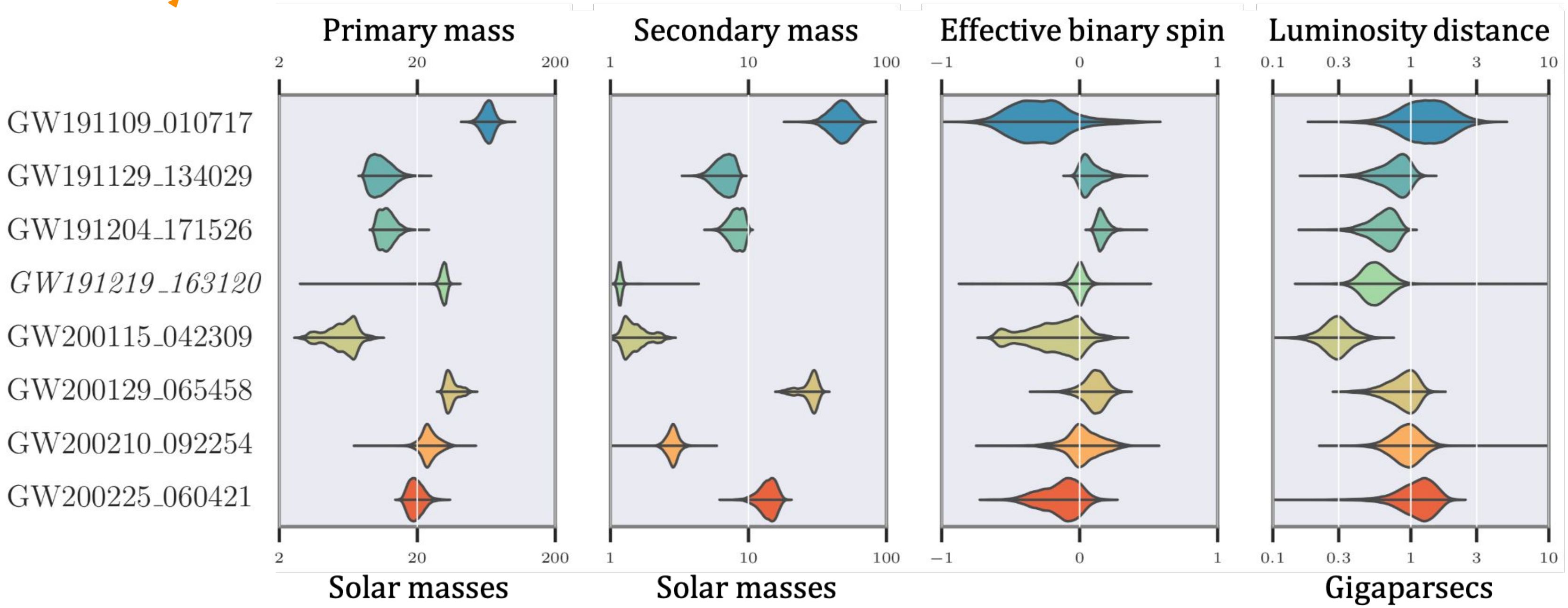

negative spin

lightest BBH in O3b

positive spin

NSBH

NSBH

misaligned spin

NSBH?

negative spin

Tables

	BNS	NSBH	BBH	NS-Gap	BBH-gap	Full
	$m_1 \in [1, 2.5]M_\odot$	$m_1 \in [2.5, 50]M_\odot$	$m_1 \in [2.5, 100]M_\odot$	$m_1 \in [2.5, 5]M_\odot$	$m_1 \in [2.5, 100]M_\odot$	$m_1 \in [1, 100]M_\odot$
	$m_2 \in [1, 2.5]M_\odot$	$m_2 \in [1, 2.5]M_\odot$	$m_2 \in [2.5, 100]M_\odot$	$m_2 \in [1, 2.5]M_\odot$	$m_2 \in [2.5, 5]M_\odot$	$m_2 \in [1, 100]M_\odot$
PDB (pair)	960^{+1740}_{-700}	59^{+81}_{-38}	$25^{+10}_{-7.0}$	41^{+69}_{-30}	$9.3^{+18.7}_{-7.6}$	1100^{+1700}_{-750}
PDB (ind)	250^{+640}_{-196}	170^{+150}_{-89}	$22^{+9.0}_{-6.0}$	29^{+55}_{-23}	$10^{+15}_{-8.0}$	470^{+830}_{-300}
MS	470^{+1430}_{-413}	57^{+123}_{-42}	42^{+88}_{-20}	$3.7^{+20.3}_{-3.4}$	$0.17^{+55.83}_{-0.16}$	650^{+1550}_{-460}
BGP	$99.0^{+260.0}_{-86.0}$	$32.0^{+62.0}_{-25.0}$	$33.0^{+16.0}_{-10.0}$	$2.1^{+33.0}_{-2.1}$	$5.1^{+12.0}_{-4.0}$	$180.0^{+260.0}_{-110.0}$
MERGED	13 – 1900	7.4 – 320	16 – 130	0.029 – 84	0.0095 – 56	71 – 2200

Tables

	$m_1 \in [5,20]M_\odot$ $m_2 \in [5,20]M_\odot$	$m_1 \in [20,50]M_\odot$ $m_2 \in [5,50]M_\odot$	$m_1 \in [50,100]M_\odot$ $m_2 \in [5,100]M_\odot$	All BBH
PP	$23.4^{+12.9}_{-8.6}$	$4.5^{+1.8}_{-1.3}$	$0.2^{+0.1}_{-0.1}$	$28.1^{+14.8}_{-10.0}$
BGP	$20.0^{+10.0}_{-8.0}$	$6.4^{+3.0}_{-2.1}$	$0.74^{+1.2}_{-0.46}$	$33.0^{+16.0}_{-10.0}$
FM	$21.1^{+10.7}_{-8.3}$	$4.1^{+2.0}_{-1.4}$	$0.2^{+0.3}_{-0.1}$	$26.0^{+11.5}_{-8.7}$
PS	$27^{+12}_{-9.4}$	$3.6^{+1.5}_{-1.1}$	$0.2^{+0.18}_{-0.1}$	$32^{+14}_{-9.6}$
MERGED	12.8 – 40	2.5 – 6.3	0.098 – 0.5	17.3 – 45

Search methods

Same methods as GWTC-2.1 (GstLAL, MBTA, PyCBC) and GWTC-2 (cWB).

Descriptions of **pipelines** are given with more details in Section IV and Appendix D of the paper.

Modeled searches

- GstLAL, MBTA, PyCBC Broad, PyCBC BBH
- Assume the source is CBC.
- Uses matched filtering and banks of template waveforms with varying parameters to find signals in the data.
- HL, HV, LV, HLV coincidences.
- GstLAL allows for single detector candidates.

Minimally modeled search

- CWB
- Can potentially identify non-CBC sources.
- Does not use matched filtering or waveforms.
- Identifies excess power in coincident strain data to find signals.
- HL, HV, LV coincidences.

Population-weighted posteriors

With growing catalog we can use the population as the prior for our event posteriors.

More details in Appendix E of the paper.

- Event posteriors reweighted with Power law + Peak (PP), Flexible Mixtures (FM)
- For some events: q~1 preferred, PP and FM models disagree (with PP model pulling distribution towards $\chi_{\rm eff} \approx 0$)

Original, PP, FM

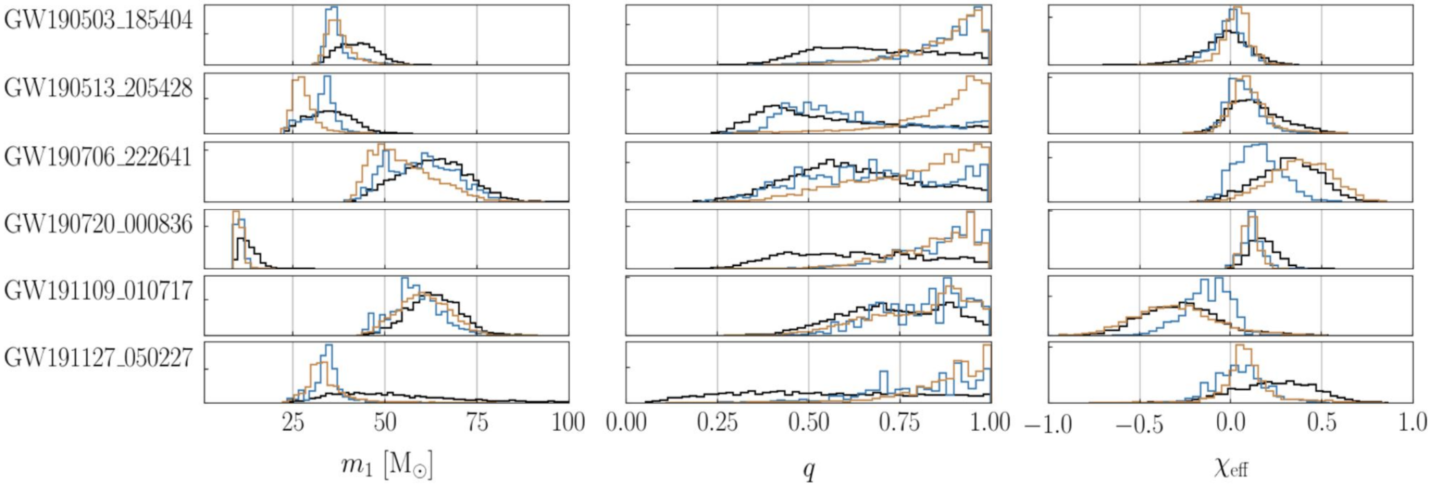

Event selection criterion

We use the **false alarm rate (FAR)** to determine which triggers we should analyze

Events with a **FAR<1/1 year** are studied in this work

Some analyses restricted to the subset of these events with **FAR<¼ years**

From our analyses, we can estimate the **probability of astrophysical origin** of any given event in future observing runs

- This work and GWTC-3 use different criteria for what constitutes a GW event
  - GWTC-3 uses the probability that a trigger is astrophysical (p_{astro})
  - We use the false alarm rate (FAR) as the metric for inclusion
- Relaxed criteria means we can analyze events like GW200105
  - Neutron star-black hole event
  - FAR of ~⅕ years, but p_{astro} of .36

- What's the difference?
  - Potential GW events are assigned a signal-to-noise ratio (SNR) based on their "loudness"
  - FAR describes how frequently background noise should make a signal with an SNR greater than the event's SNR
  - Using a population model, we can estimate how frequently binaries with a given combination of masses and spins are observed
  - Using this event rate and FAR, we compute p_{astro} for a given GW event